



Since January 2020 Elsevier has created a COVID-19 resource centre with free information in English and Mandarin on the novel coronavirus COVID-19. The COVID-19 resource centre is hosted on Elsevier Connect, the company's public news and information website.

Elsevier hereby grants permission to make all its COVID-19-related research that is available on the COVID-19 resource centre - including this research content - immediately available in PubMed Central and other publicly funded repositories, such as the WHO COVID database with rights for unrestricted research re-use and analyses in any form or by any means with acknowledgement of the original source. These permissions are granted for free by Elsevier for as long as the COVID-19 resource centre remains active.



Novel fractional order SIDARTHE mathematical model of COVID-19 pandemic



M. Higazy^{a,b}

^aDepartment of Mathematics and Statistics, Faculty of Science, Taif University, Saudi Arabia

^bDepartment of Physics and Engineering Mathematics, Faculty of Electronic Engineering, Menoufia University, Menouf, Egypt

ARTICLE INFO

Article history:

Received 28 May 2020

Revised 11 June 2020

Accepted 12 June 2020

Available online 13 June 2020

MSC:

41A28

65D05

65H10

65L20

65P30

65P40

65Z05

Keywords:

COVID-19

Coronavirus disease

Fractional order sidarthe model

Fractional optimal control

Lyapunov exponents

Predictor-corrector algorithms for fractional differential equations

ABSTRACT

Nowadays, COVID-19 has put a significant responsibility on all of us around the world from its detection to its remediation. The globe suffer from lockdown due to COVID-19 pandemic. The researchers are doing their best to discover the nature of this pandemic and try to produce the possible plans to control it. One of the most effective method to understand and control the evolution of this pandemic is to model it via an efficient mathematical model. In this paper, we propose to model COVID-19 pandemic by fractional order SIDARTHE model which did not appear in the literature before. The existence of a stable solution of the fractional order COVID-19 SIDARTHE model is proved and the fractional order necessary conditions of four proposed control strategies are produced. The sensitivity of the fractional order COVID-19 SIDARTHE model to the fractional order and the infection rate parameters are displayed. All studies are numerically simulated using MATLAB software via fractional order differential equation solver.

© 2020 Elsevier Ltd. All rights reserved.

1. Introduction

All the world states' governments introduce a big effort and vital measures to eliminate the outbreak of COVID-19 [22]. COVID-19 is a new progeny of coronavirus, SARS-CoV-2 and firstly detected in Wuhan, China [52,57]. In the few months after discovering it, the number of patients were increasing exponentially. The taken measures against COVID-19 until the day of writing these words didn't prevent the growth of infected cases around the globe. The World Health Organization situation report published in 25 May 2020 informed that 5,304,772 cases as total cases and 342,029 deaths around the globe [54].

Using mathematical model to predict the epidemics is very useful in order to understand the nature of the epidemic and to design an efficient strategies to control it [4,8,14,26,27].

It is common to study the humanitarian diffusion of epidemics via SIR or SEIR models [11,13,33,48]. Various models have been

proposed to model and study COVID-19 pandemic. Taking into account the risk understanding and the accumulative issue of cases, COVID-19 pandemic has been modeled by Lin et al. via extending SEIR model [38] where S signifies the susceptible, E signifies the exposed, I signifies the infected and R signifies the removed cases. In [3], Anastassopoulou et al. have suggested the SIR model in the discrete time mode taking into account the dead cases. In [9] by Casella, SIR model is expanded to study the delays effect and to compare the policies of containment. In [56] by Wu et al., the COVID-19 severity has been estimated using the dynamics of transition. In [25,34], random transition models have been studied. In [12], the general multi-group SEIRA model was represented and numerically tested for modeling the diffusion of COVID-19 between a non-homogeneous population. The basic mathematical tool used to model several epidemics is differential equations in various modes (ordinary, fractional, with delay, randomly detected or partial) [27-29].

Many research efforts have been widely done to control the outbreaks of epidemics via optimal control [20,44-47]. The optimal

E-mail addresses: m.higazy@tu.edu.sa, mahmoudhegazy380@hotmail.com

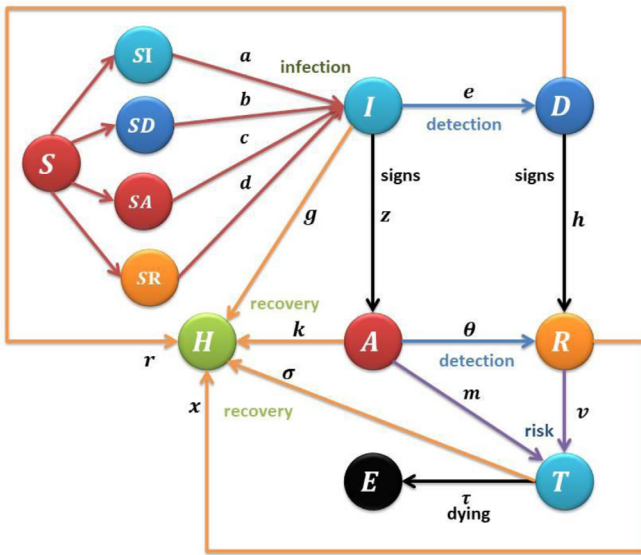


Fig. 1. Eight phases of COVID-19 epidemic interactions digraph ($\bar{\Psi}$) where S , I , D , A , R , T , H and E signify the population fractions explained in Table 1 where the sub-phases SI , SD , SA , SR are appeared.

control idea is to look for the utmost powerful plan that decreases the rate of infection to a possible minimum limit with optimal minimum cost of circulating a treatment or preventative inoculation [39,44-47,51]. These plans may include treatments, inoculation with vaccines, social distances, educational programs [6,10].

Studying the epidemiological diseases mathematically become very important [6,7,16,17,37,40]. The literature has several studies to control for example models of HIV [24], dengue fever [2], tuberculosis [50], delayed SIR [1] and delayed SIRS [29,58].

The fractional order differential equations add an extra dimensions in the study of dynamics of epidemiological models. Therefore the fractional version of many epidemical models have been investigated as in [29–32,39,41] and [53].

Here, a new epidemiological fractional mathematical model for the COVID-19 epidemic is proposed as an extension of the classical SIR model, similar to that introduced by Gumel et al. for SARS in [23] and as a generalization of SIDARTHE model proposed in [21]. As explained in Section 3, in SIDARTHE model, the infected cases are classified into five different classes depending on the detection and the appearance of symptoms [21].

In this work, we consider the fractional order SIDARTHE model and then we derive the fractional order necessary conditions for existence of a stable solution. In addition, we study an optimal control plans for the fractional order SIDARTHE model via four control strategies that include the availability of vaccination and existence of treatments for the infected detected three population fraction phases. Applying the fractional order differential equations numerical solver using MATLAB software, we show the dynamics of the state variables of the model and display the effect of changing the fractional derivative order on the system response. Also, the effect of changing the infection rates on the fractional order SIDARTHE model's state variables. We also implement the optimal control strategies numerically for the fractional order SIDARTHE model.

The remaining parts of the paper are organized as follows. In Section 2, Preliminaries and basic definition of the fractional derivative are introduced. Describing COVID-19 epidemic SIDARTHE fractional mathematical model is introduced in Section 3. The details of the optimal control strategy and its implementation are given in Section 4. Numerical simulations of the uncontrolled frac-

tional order SIDARTHE model, the effects of changing the fractional derivative order on the system response and the effects of changing the infection rates are all given in [Section 5](#). Numerical simulations of the controlled fractional order SIDARTHE model and the effects of applying the proposed control strategies are represented in [Section 6](#). The concluding remarks are put in [Section 7](#) followed by the list of cited references.

2. Preliminaries

Many definitions of fractional order derivatives exist such as Riemann-Liouville's derivative, Grunwald Letnikov's derivative, Caputo's derivative, Caputo-Fabrizio, Atangana-Baleanu, etc. The interested reader can consult for example [42,43] and the references therein for more details about fractional order definitions with applications. We have used Caputo's definition throughout the paper. Caputo fractional derivative operator Δ^q of order q (see [18,30,39,42,43,49]) is defined as:

$\Delta^q f(t) = \frac{1}{\Gamma(n-q)} \int_0^t \frac{f^{(n)}(x)}{(t-x)^{q-n+1}} dx$, $t > 0$, $q > 0$, $n-1 < \eta \leq n$, where $F(\cdot)$ generalizes the Gamma function. For more

n , $n \in N$, where $\Gamma(\cdot)$ symbolizes the Gamma function. For more details about the basic definitions and characteristics of fractional derivatives see [18,30,39,49].

Notation: For numerical simulations, the predictor-corrector PECE method of Adams-Bashforth-Moulton type described in details in [15,19] has been utilized and programmed with MATLAB software.

3. COVID-19 epidemic SIDARTHE fractional mathematical model

Giulia Giordano et al. in [21] modeled COVID-19 epidemic via SIDARTHE model and compare its response with the real data in Italy. SIDARTHE model distinguishes between determined infected cases and undetermined infected cases and between various degrees of illness (DOI). In SIDARTHE COVID-19 epidemic model, the total population is partitioned into eight phases of malady as recorded in the Table 1. Fig. 1 shows the interaction graph ($\bar{\Psi}$) between the eight phases of malady. In Fig. 1, the susceptible population partition S is partitioned into four sub-phases to show the hidden sub-phases of the susceptible population partition S , namely SI, SD, SA and SR . The detailed interaction digraph in Fig. 1 is named $\bar{\Psi}$ that may be studied using graph theory tools to discover more features about the model.

COVID-19 epidemic SIDARTHE model is described mathematically by eight ordinary differential equations [21].

The deterministic characteristic is essential in modeling the epidemics transition phenomena; the fractional derivative is very useful in modeling the epidemics transition systems because they consider the memory effect and the universal properties of the system, that are primary in the deterministic feature. The system is said to have a memory effect if its future states depend on its current states and the history of the states, and the fractional operator has this memory effect feature so it is very helpful in modeling COVID-19 diffusion model. Here, as recorded in Eqs. (3.1) to (3.8), the dynamics of the population in each phase with time is described with eight fractional order (q) differential equations:

$$\Delta^q S(t) = -aSI - bSD - cSA - dSR \quad (3.1)$$

$$\Delta^q I(t) = aSI + bSD + cSA + dSR - eI - zI - gl \quad (3.2)$$

$$\Delta^q D(t) = eI - hD - rD \quad (3.3)$$

$$\Delta^q A(t) = zI - \theta A - mA - kA \quad (3.4)$$

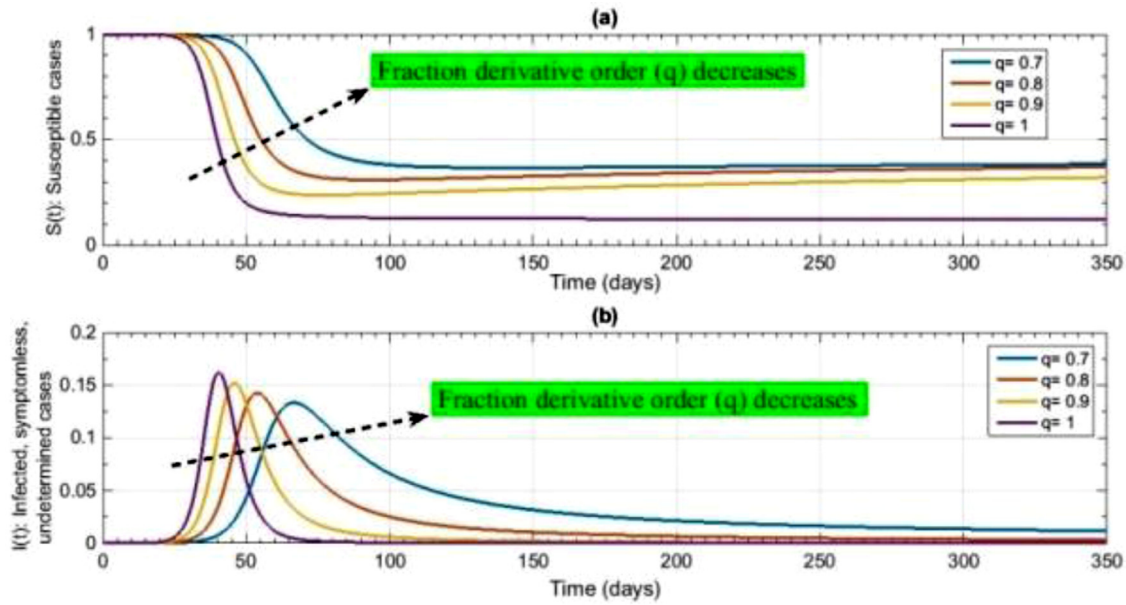


Fig. 2. The time history of Susceptible cases ($S(t)$) and Infected, symptomless, undetermined cases ($I(t)$) with different fractional derivative order (q): (a) time history of $S(t)$ with $q = 0.7, 0.8, 0.9, 1$; (b) time history of $I(t)$ with $q = 0.7, 0.8, 0.9, 1$.

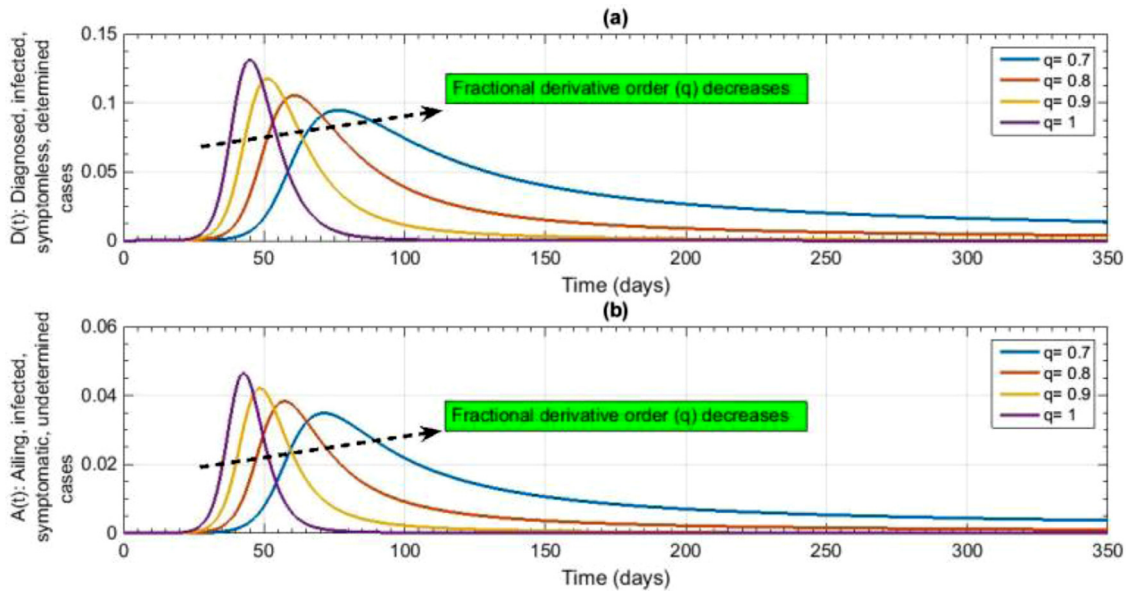


Fig. 3. The time history of Diagnosed, infected, symptomless, determined cases ($D(t)$) and Ailing, infected, symptomatic, undetermined cases ($A(t)$) with different fractional derivative order (q): (a) time history of $D(t)$ with $q = 0.7, 0.8, 0.9, 1$; (b) time history of $A(t)$ with $q = 0.7, 0.8, 0.9, 1$.

Table 1
Eight phases of population modeling COVID-19 epidemic.

| Model symbol | Phase of malady |
|--------------|---|
| S | Susceptible (not sick) population fraction. |
| I | Infected (symptomless, undetermined) population fraction. |
| D | Diagnosed (infected, symptomless, determined) population fraction. |
| A | Ailing (infected, with symptoms undetermined) population fraction. |
| R | Recognized (infected, with symptoms, determined) population fraction. |
| T | Threatened (infected, with life-menacing symptoms, determined) population fraction. |
| H | Healed (recuperate) population fraction. |
| E | Extinct (died out) population fraction. |

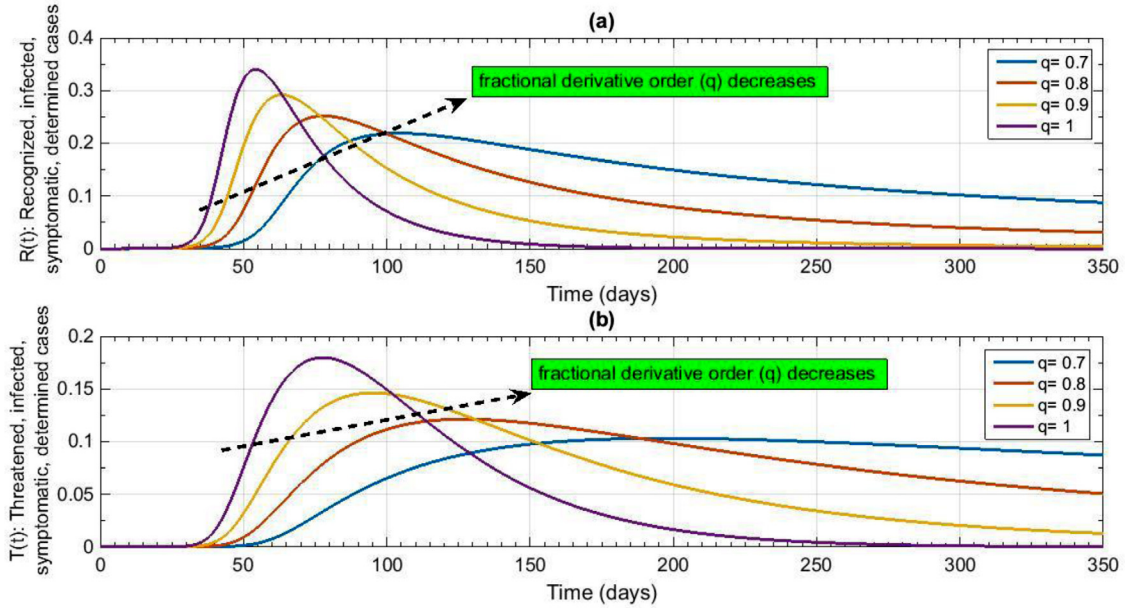


Fig. 4. The time history of Recognized, infected, symptomatic, determined cases ($R(t)$) and Threatened, infected, symptomatic, determined cases ($T(t)$) with different fractional derivative order (q): (a) time history of $R(t)$ with $q = 0.7, 0.8, 0.9, 1$; (b) time history of $T(t)$ with $q = 0.7, 0.8, 0.9, 1$.

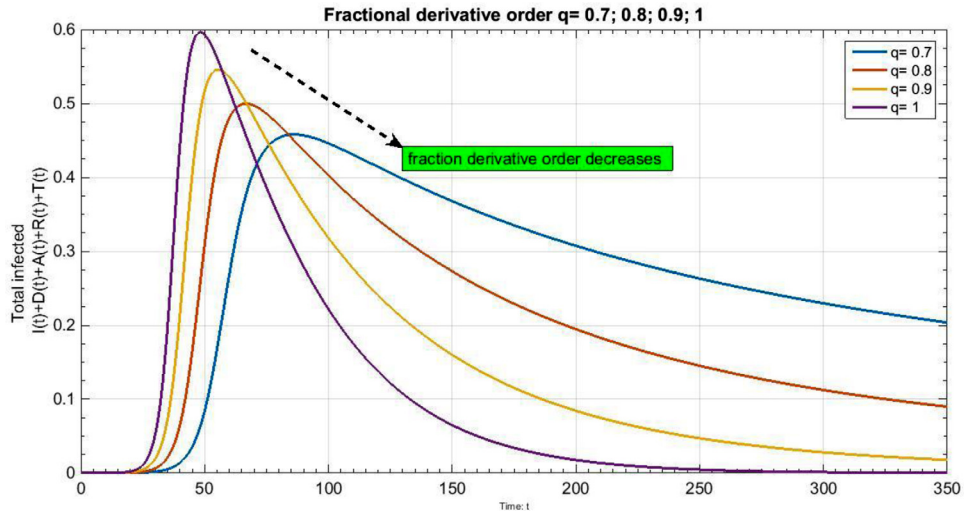


Fig. 5. The time history of the total infected cases: $I(t) + D(t) + A(t) + R(t) + T(t)$, with different fractional derivative order $q = 0.7, 0.8, 0.9, 1$.

$$\Delta^q R(t) = hD + \theta A - \nu R - xR \quad (3.5)$$

$$\Delta^q T(t) = mA + \nu R - \sigma T - \tau T \quad (3.6)$$

$$\Delta^q H(t) = gI + rD + kA + xR + \sigma T \quad (3.7)$$

$$\Delta^q E(t) = \tau T \quad (3.8)$$

Where the population fraction in each phase is modeled by a state variable that is represented by an uppercase English letters S, I, D, A, R, T, H and E . In the SIDARTHE model (3.1) to (3.8), the parameters are symbolized by small Greek and English letters. All model parameters are positive numbers and have been estimated in [21] using the real data. Fig. 1 shows the impact of each different phases of epidemic graphically. The SIDARTHE Covid-19 model parameters have the following real meaning:

- a signifies the rate of infection as a result of contacting among a susceptible case and an infected case.
- b signifies the rate of infection as a result of contacting among a susceptible case and a diagnosed case.
- c signifies the rate of infection as a result of contacting among a susceptible case and an ailing case.
- d signifies the rate of infection as a result of contacting among a susceptible case and a recognized case.
- e signifies the detection probability rate of infected symptomless cases.
- θ signifies the detection probability rate of infected with symptoms cases.
- z signifies the rate of probability at which an infected case is not conscious of becoming infected.
- h signifies the rate of probability at which an infected case is conscious of becoming infected.
- m signifies the rate at which undetermined infected case develops life-menacing signs.

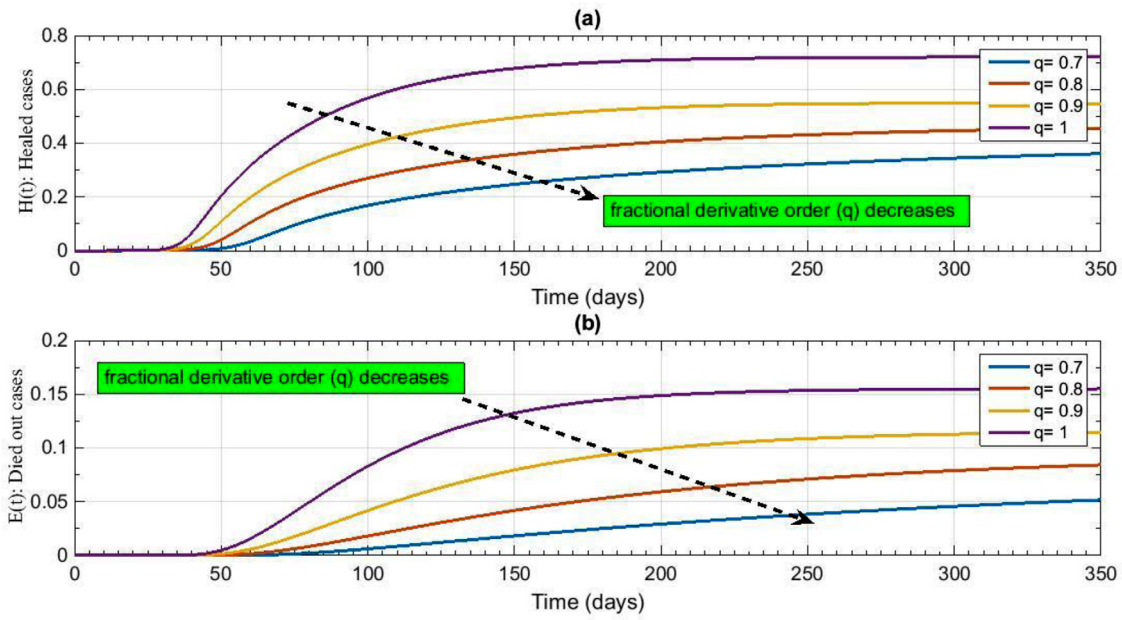


Fig. 6. The time history of Healed cases ($H(t)$) and Died out (Extinct) cases ($E(t)$) with different fractional derivative order (q): (a) time history of $R(t)$ with $q = 0.7, 0.8, 0.9, 1$; (b) time history of $T(t)$ with $q = 0.7, 0.8, 0.9, 1$.

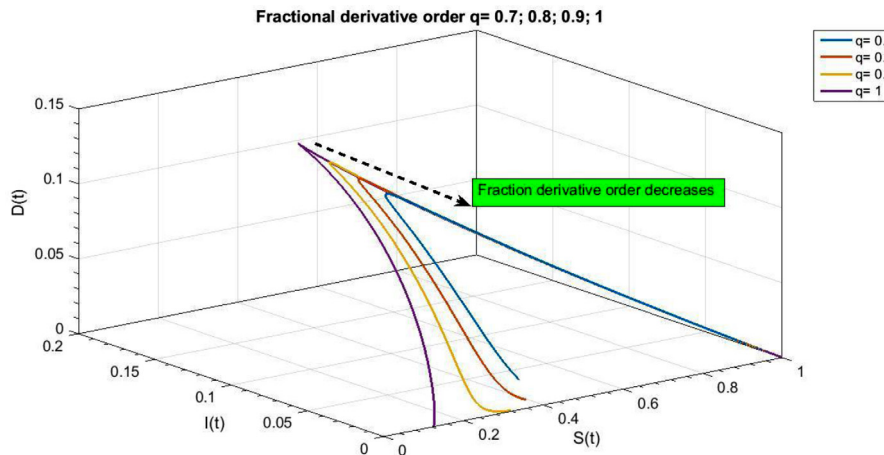


Fig. 7. Three-dimensions plot of the state variables: Diagnosed, infected, symptomless, determined cases ($D(t)$), Infected, symptomless, undetermined cases ($I(t)$) and Susceptible cases ($S(t)$) with different fractional derivative order $q = 0.7, 0.8, 0.9, 1$.

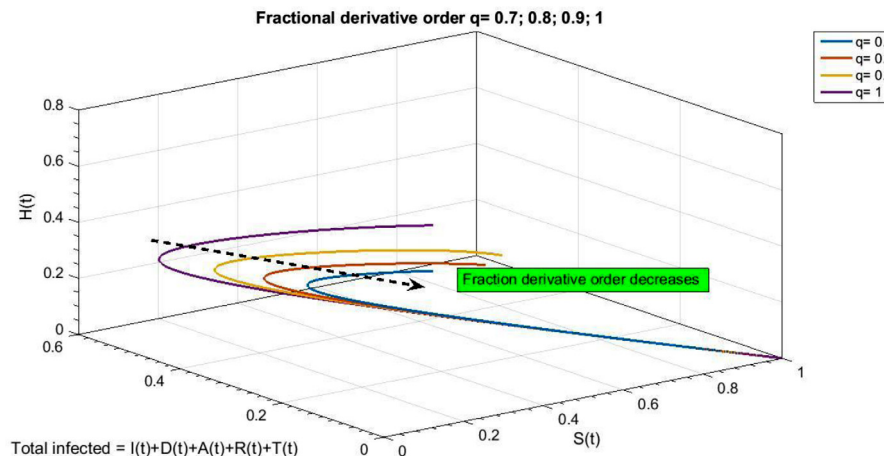


Fig. 8. Three-dimensions plot of the state variables: Healed cases ($H(t)$), Total infected ($I(t) + D(t) + A(t) + R(t) + T(t)$) and Susceptible cases ($S(t)$) with different fractional derivative order $q = 0.7, 0.8, 0.9, 1$.

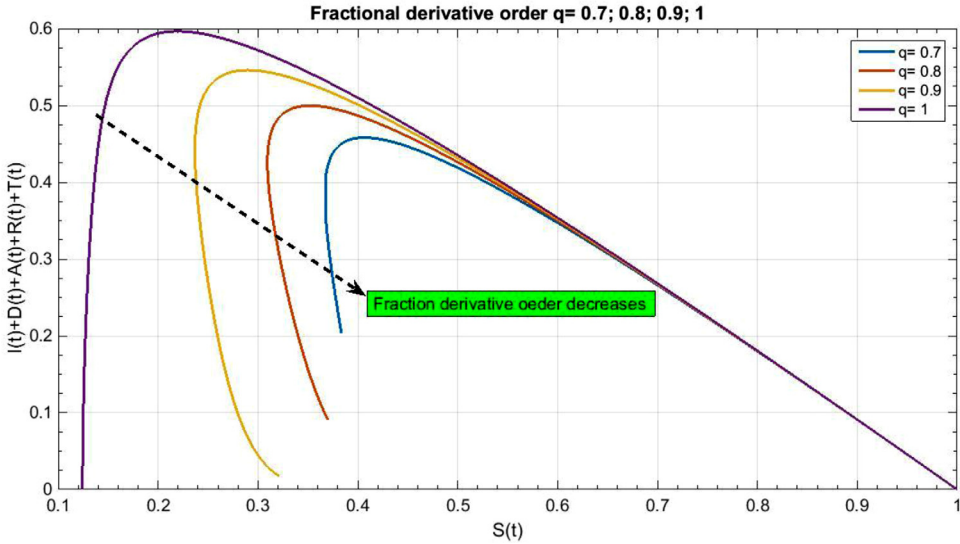


Fig. 9. The phase plane of state variables: Total infected ($I(t) + D(t) + A(t) + R(t) + T(t)$) and susceptible cases ($S(t)$) with different fractional derivative order $q = 0.7, 0.8, 0.9, 1$.

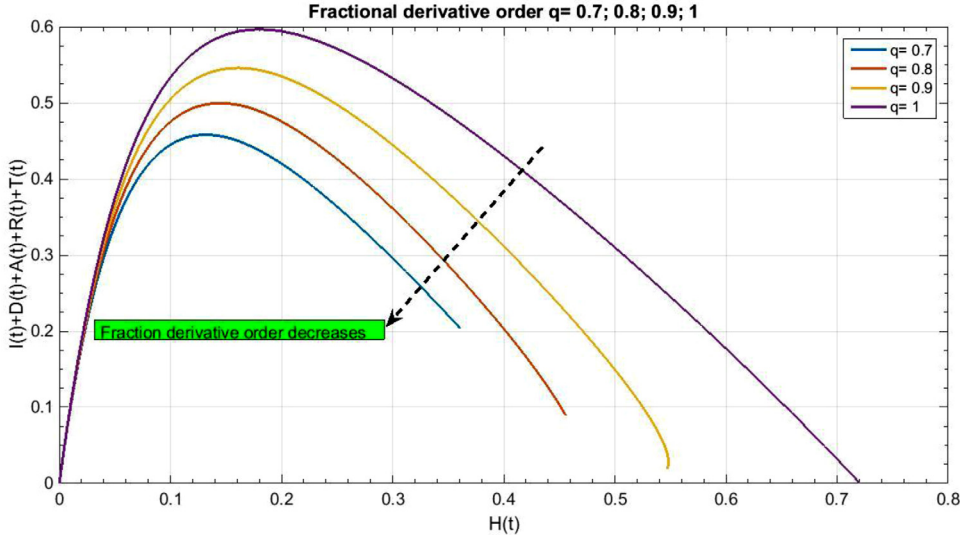


Fig. 10. The phase plane of state variables: Total infected $TI(t) = I(t) + D(t) + A(t) + R(t) + T(t)$ and Healed cases ($H(t)$) with different fractional derivative order $q = 0.7, 0.8, 0.9, 1$.

- v signifies the rate at which the determined infected case develops life-menacing signs.
- τ signifies the death rate (for infected cases with life-menacing signs).
- g, k, x, r and σ signify the rate of healing for the five phases of infected cases.

For more details about the model choices see [21] and the references cited there.

3.1. SIDARTHE fractional order mathematical model discussion

From Eqs. (3.1) to (3.8) and since the states $H(t)$ and $E(t)$ are sink vertices in the model graph Ψ (see Fig. 1), then they are considered as accumulative state variables that rely only on their own starting situations and the other state variables.

Since summing up all Eqs. (3.1) to (3.8) gives zero as a result then the system is compartmentalized and shows the conservation property of mass: as can be directly proved,

$$D^q S(t) + D^q I(t) + D^q D(t) + D^q A(t) + D^q R(t) + D^q T(t) + D^q H(t) + D^q E(t) = 0 \quad (3.9)$$

Which implies that the total population (the sum of all state variables) is constant. Let

$$X = [S(t), I(t), D(t), A(t), R(t), T(t), H(t), E(t)]^{tr} \quad (3.10)$$

be the state variables vector. Since the state variables signify the population fractions, we can suppose that $\sum_i X(i) = 1$, such that 1 signifies the total population, dead are included.

3.2. Existence of uniformly stable solution of COVID-19 epidemic SIDARTHE fractional mathematical model

Assume that

$$\Delta^q S(t) = -aSI - bSD - cSA - dSR = f_1(S, I, D, A, R, T, H, E) \quad (3.11)$$

$$\Delta^q I(t) = aSI + bSD + cSA + dSR - eI - zI - gI = f_2(S, I, D, A, R, T, H, E) \quad (3.12)$$

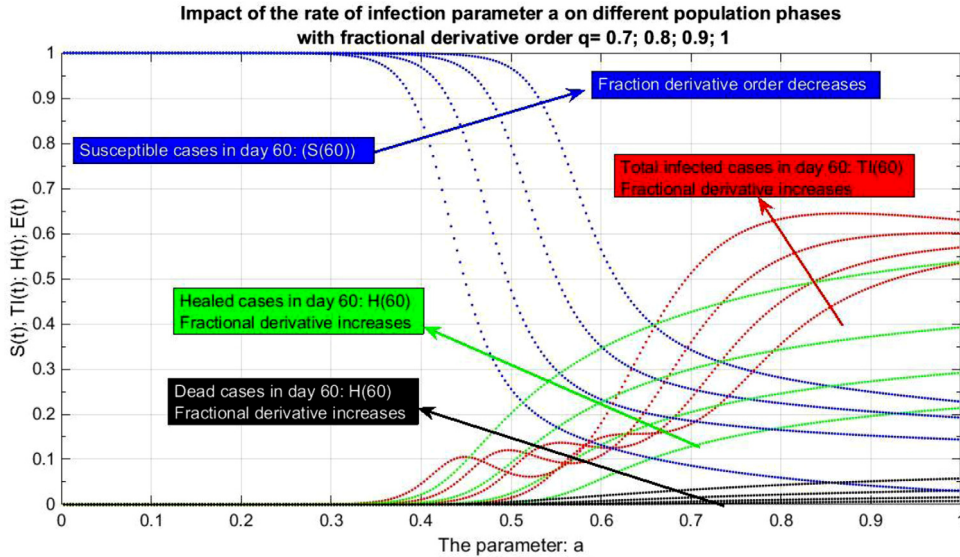


Fig. 11. The effect of changing the rate of infection (parameter a) on different population phases at day 60 with different fractional derivative order $q = 0.7, 0.8, 0.9, 1$.

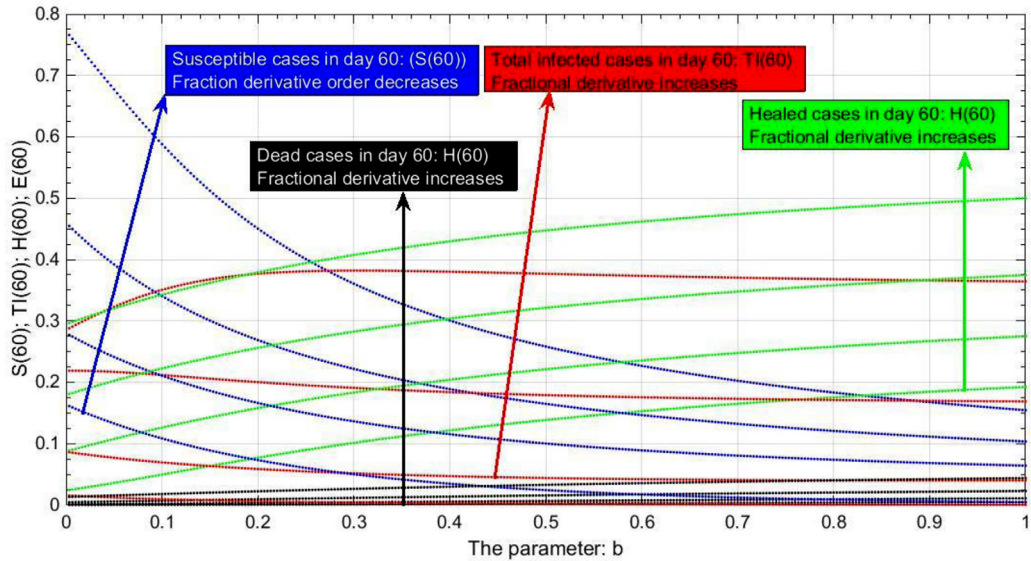


Fig. 12. The effect of changing the rate of infection (parameter b) on different population phases at day 60 with different fractional derivative order $q = 0.7, 0.8, 0.9, 1$.

$$\Delta^q D(t) = el - hD - rD = f_3(S, I, D, A, R, T, H, E) \quad (3.13)$$

$$\Delta^q E(t) = \tau T = f_8(S, I, D, A, R, T, H, E) \quad (3.18)$$

Assume for a constant N that

$$\Omega = \{(S(t), I(t), D(t), A(t), R(t), T(t), H(t), E(t)) \in \mathbb{R}^8 : |X(i)| \leq N \text{ and } t \in [0, T]\}.$$

Then over Ω , we have

$$\begin{aligned} \frac{\partial f_1}{\partial S} &= -al - bD - cA - dR \Rightarrow \left| \frac{\partial f_1}{\partial S} \right| = al + bD + cA + dR \leq k_{11}; \\ \frac{\partial f_1}{\partial I} &= -aS \Rightarrow \left| \frac{\partial f_1}{\partial I} \right| = aS \leq k_{12}; \quad \frac{\partial f_1}{\partial D} = -bS \Rightarrow \left| \frac{\partial f_1}{\partial D} \right| = bS \leq k_{13}; \\ \frac{\partial f_1}{\partial A} &= -cS \Rightarrow \left| \frac{\partial f_1}{\partial A} \right| = cS \leq k_{14}; \quad \frac{\partial f_1}{\partial R} = -dS \Rightarrow \left| \frac{\partial f_1}{\partial R} \right| = dS \leq k_{15}; \\ \frac{\partial f_1}{\partial T} &= 0 \Rightarrow f_1(T) = k_{16}; \quad \frac{\partial f_1}{\partial H} = 0 \Rightarrow f_1(H) = k_{17}; \quad \frac{\partial f_1}{\partial E} = 0 \Rightarrow f_1(E) = k_{18}; \end{aligned} \quad (3.19)$$

$$\Delta^q A(t) = zI - \theta A - mA - kA = f_4(S, I, D, A, R, T, H, E) \quad (3.14)$$

$$\Delta^q R(t) = hD + \theta A - vR - xR = f_5(S, I, D, A, R, T, H, E) \quad (3.15)$$

$$\Delta^q T(t) = mA + vR - \sigma T - \tau T = f_6(S, I, D, A, R, T, H, E) \quad (3.16)$$

$$\Delta^q H(t) = gI + rD + kA + xR + \sigma T = f_7(S, I, D, A, R, T, H, E) \quad (3.17)$$

$$\begin{aligned} \frac{\partial f_2}{\partial S} &= al + bD + cA + dR \Rightarrow \left| \frac{\partial f_2}{\partial S} \right| = al + bD + cA + dR \leq k_{21}; \\ \frac{\partial f_2}{\partial I} &= aS - (e + z + g) \Rightarrow \left| \frac{\partial f_2}{\partial I} \right| = aS + (e + z + g) \leq k_{22}; \quad \frac{\partial f_2}{\partial D} = bS \Rightarrow \left| \frac{\partial f_2}{\partial D} \right| = bS \leq k_{23}; \\ \frac{\partial f_2}{\partial A} &= cS \Rightarrow \left| \frac{\partial f_2}{\partial A} \right| = cS \leq k_{24}; \quad \frac{\partial f_2}{\partial R} = dS \Rightarrow \left| \frac{\partial f_2}{\partial R} \right| = dS \leq k_{25}; \\ \frac{\partial f_2}{\partial T} &= 0 \Rightarrow f_2(T) = k_{26}; \quad \frac{\partial f_2}{\partial H} = 0 \Rightarrow f_2(H) = k_{27}; \quad \frac{\partial f_2}{\partial E} = 0 \Rightarrow f_2(E) = k_{28}. \end{aligned} \quad (3.20)$$

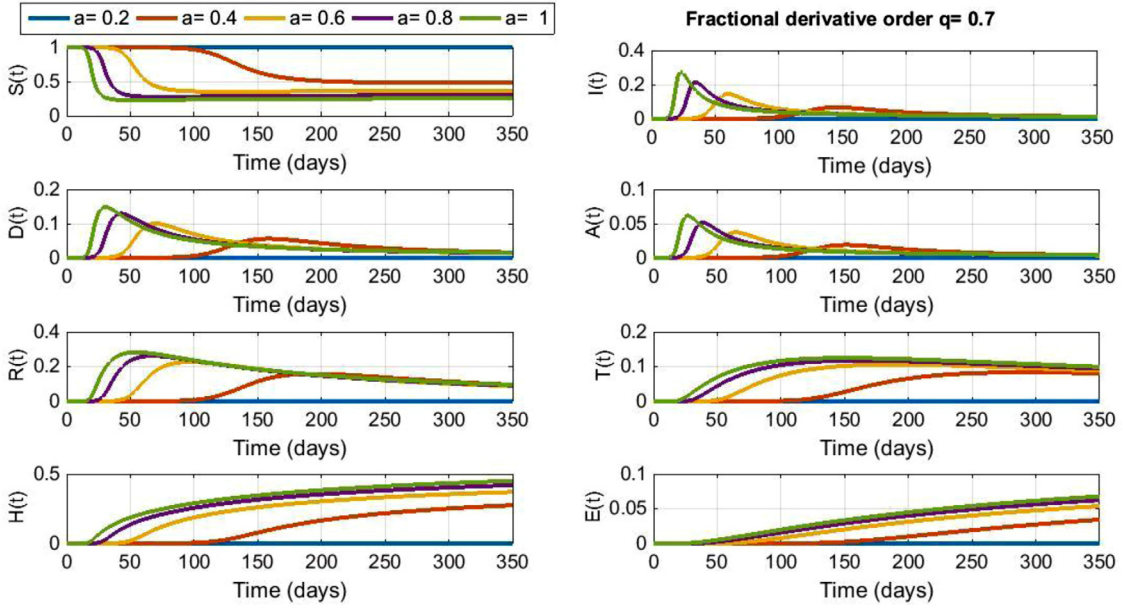


Fig. 13. The effect of changing the rate of infection (parameter a) on all population phases over time where the fractional derivative order $q = 0.7$.

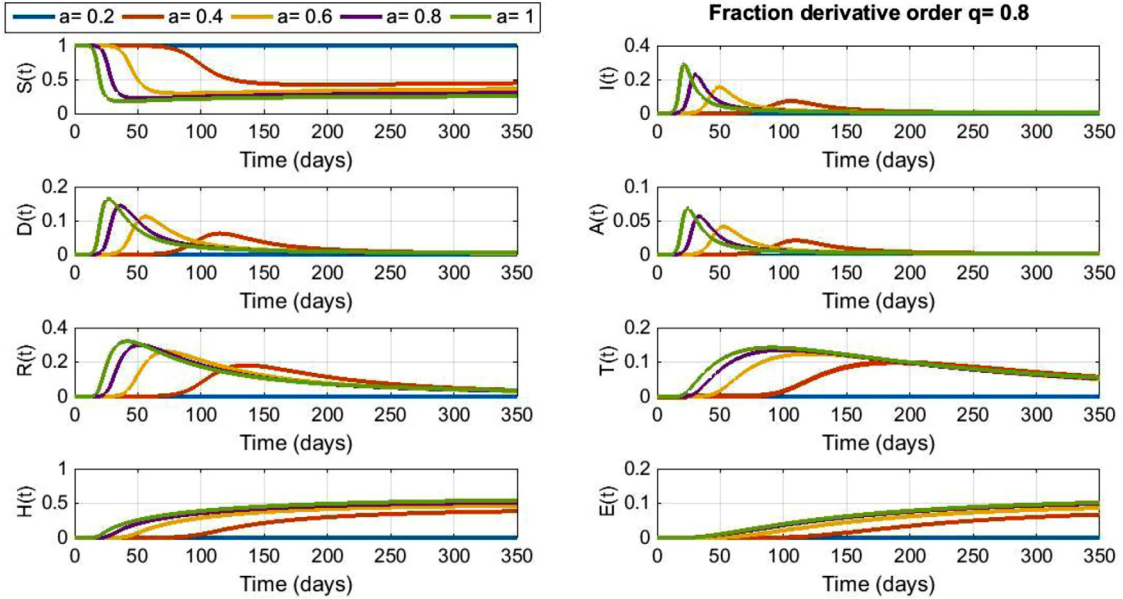


Fig. 14. The effect of changing the rate of infection (parameter a) on all population phases over the time where the fractional derivative order $q = 0.8$.

$$\begin{aligned} \frac{\partial f_3}{\partial S} = 0 \Rightarrow f_3(S) = k_{31}; \quad \frac{\partial f_3}{\partial I} = e \Rightarrow \left| \frac{\partial f_3}{\partial I} \right| \leq k_{32}; \\ \frac{\partial f_3}{\partial D} = -h - r \Rightarrow \left| \frac{\partial f_3}{\partial D} \right| = h + r \leq k_{33}; \quad \frac{\partial f_3}{\partial A} = 0 \Rightarrow f_3(A) = k_{34}; \\ \frac{\partial f_3}{\partial R} = 0 \Rightarrow f_3(R) = k_{35}; \quad \frac{\partial f_3}{\partial T} = 0 \Rightarrow f_3(T) = k_{36}; \quad \frac{\partial f_3}{\partial H} = 0 \Rightarrow f_3(H) = k_{37}; \\ \frac{\partial f_3}{\partial E} = 0 \Rightarrow f_3(E) = k_{38}. \end{aligned} \quad (3.21)$$

$$\begin{aligned} \frac{\partial f_5}{\partial S} = 0 \Rightarrow f_5(S) = k_{51}; \quad \frac{\partial f_5}{\partial I} = 0 \Rightarrow f_5(I) = k_{52}; \\ \frac{\partial f_5}{\partial D} = h \Rightarrow \left| \frac{\partial f_5}{\partial D} \right| \leq k_{53}; \quad \frac{\partial f_5}{\partial A} = \theta \Rightarrow \left| \frac{\partial f_5}{\partial A} \right| \leq k_{54}; \\ \frac{\partial f_5}{\partial R} = -v - x \Rightarrow \left| \frac{\partial f_5}{\partial R} \right| \leq k_{55}; \quad \frac{\partial f_5}{\partial T} = 0 \Rightarrow f_5(T) = k_{56}; \quad \frac{\partial f_5}{\partial H} = 0 \Rightarrow f_5(H) = k_{57}; \\ \frac{\partial f_5}{\partial E} = 0 \Rightarrow f_5(E) = k_{58}. \end{aligned} \quad (3.23)$$

$$\begin{aligned} \frac{\partial f_4}{\partial S} = 0 \Rightarrow f_4(S) = k_{41}; \quad \frac{\partial f_4}{\partial I} = z \Rightarrow \left| \frac{\partial f_4}{\partial I} \right| \leq k_{42}; \\ \frac{\partial f_4}{\partial D} = 0 \Rightarrow f_4(S) = k_{43}; \quad \frac{\partial f_4}{\partial A} = -\theta - m - k \Rightarrow \left| \frac{\partial f_4}{\partial A} \right| \leq k_{44}; \\ \frac{\partial f_4}{\partial R} = 0 \Rightarrow f_4(R) = k_{45}; \quad \frac{\partial f_4}{\partial T} = 0 \Rightarrow f_4(T) = k_{46}; \quad \frac{\partial f_4}{\partial H} = 0 \Rightarrow f_4(H) = k_{47}; \\ \frac{\partial f_4}{\partial E} = 0 \Rightarrow f_4(E) = k_{48}. \end{aligned} \quad (3.22)$$

$$\begin{aligned} \frac{\partial f_6}{\partial S} = 0 \Rightarrow f_6(S) = k_{61}; \quad \frac{\partial f_6}{\partial I} = 0 \Rightarrow f_6(I) = k_{62}; \\ \frac{\partial f_6}{\partial D} = 0 \Rightarrow f_6(D) = k_{63}; \quad \frac{\partial f_6}{\partial A} = m \Rightarrow \left| \frac{\partial f_6}{\partial A} \right| \leq k_{64}; \\ \frac{\partial f_6}{\partial R} = v \Rightarrow \left| \frac{\partial f_6}{\partial R} \right| \leq k_{65}; \quad \frac{\partial f_6}{\partial T} = -\sigma - \tau \Rightarrow \left| \frac{\partial f_6}{\partial T} \right| \leq k_{66}; \quad \frac{\partial f_6}{\partial H} = 0 \Rightarrow f_6(H) = k_{67}; \\ \frac{\partial f_6}{\partial E} = 0 \Rightarrow f_6(E) = k_{68}. \end{aligned} \quad (3.24)$$

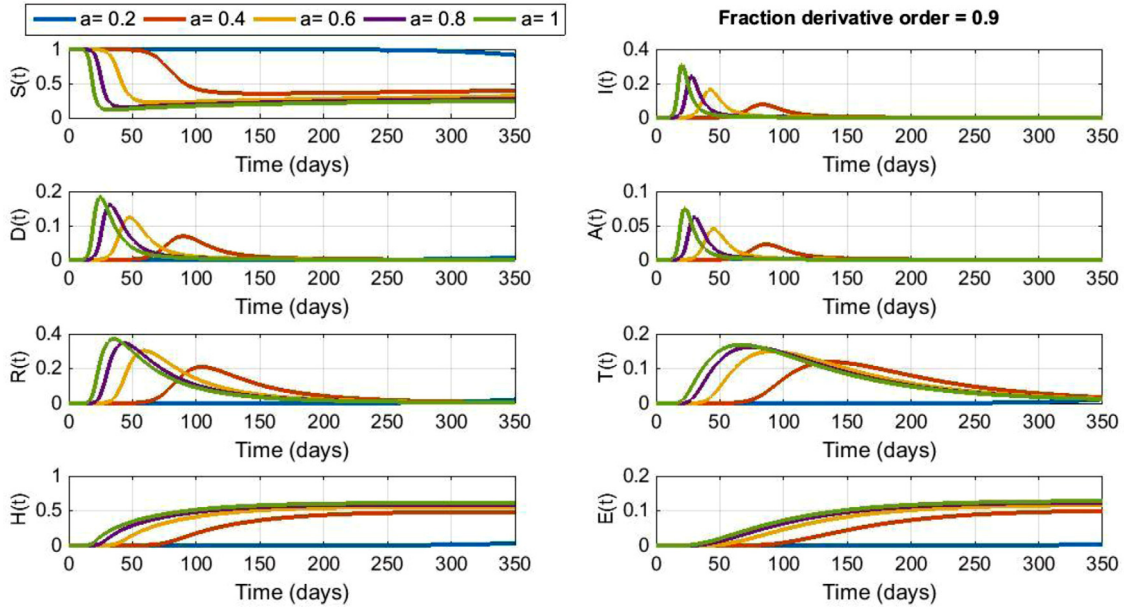


Fig. 15. The effect of changing the rate of infection (parameter a) on all population phases over the time where the fractional derivative order $q = 0.9$.

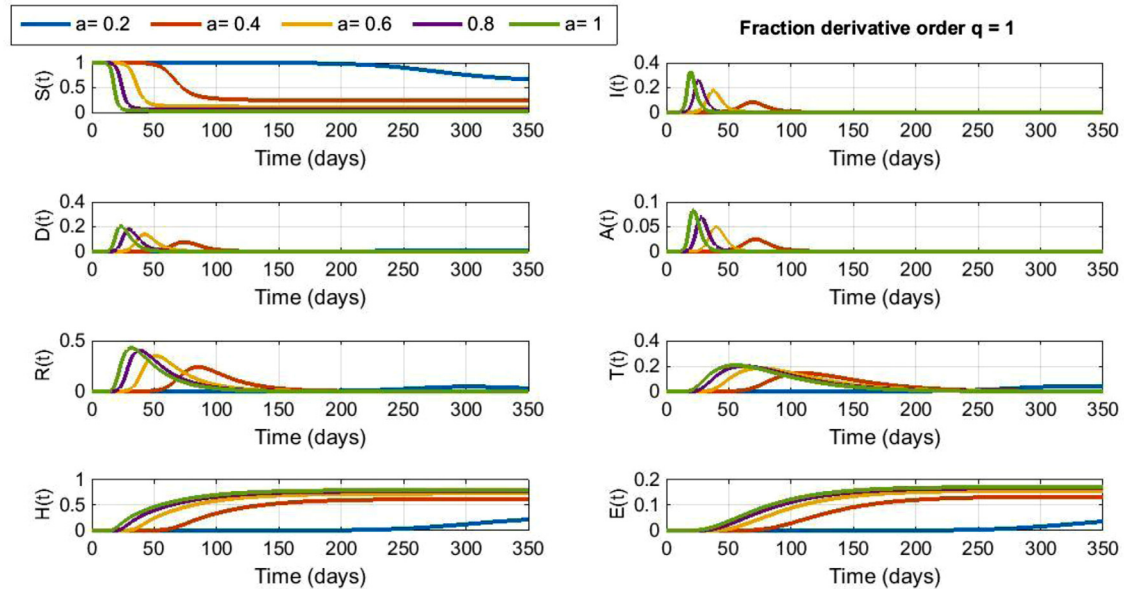


Fig. 16. The effect of changing the rate of infection (parameter a) on all population phases over the time where the fractional derivative order $q = 1$.

$$\begin{aligned} \frac{\partial f_7}{\partial S} = 0 \Rightarrow f_7(S) = k_{71}; \quad \frac{\partial f_7}{\partial I} = g \Rightarrow \left| \frac{\partial f_7}{\partial I} \right| \leq k_{72}; \\ \frac{\partial f_7}{\partial D} = r \Rightarrow \left| \frac{\partial f_7}{\partial D} \right| \leq k_{73}; \quad \frac{\partial f_7}{\partial A} = k \Rightarrow \left| \frac{\partial f_7}{\partial A} \right| \leq k_{74}; \\ \frac{\partial f_7}{\partial R} = x \Rightarrow \left| \frac{\partial f_7}{\partial R} \right| \leq k_{75}; \quad \frac{\partial f_7}{\partial T} = \sigma \Rightarrow \left| \frac{\partial f_7}{\partial T} \right| \leq k_{76}; \quad \frac{\partial f_7}{\partial H} = 0 \Rightarrow f_7(H) = k_{77}; \\ \frac{\partial f_7}{\partial E} = 0 \Rightarrow f_7(E) = k_{78}. \end{aligned} \quad (3.25)$$

$$\begin{aligned} \frac{\partial f_8}{\partial S} = 0 \Rightarrow f_8(S) = k_{81}; \quad \frac{\partial f_8}{\partial I} = 0 \Rightarrow f_8(I) = k_{82}; \\ \frac{\partial f_8}{\partial D} = 0 \Rightarrow f_8(D) = k_{83}; \quad \frac{\partial f_8}{\partial A} = 0 \Rightarrow f_8(A) = k_{84}; \\ \frac{\partial f_8}{\partial R} = 0 \Rightarrow f_8(R) = k_{85}; \quad \frac{\partial f_8}{\partial T} = \tau \Rightarrow \left| \frac{\partial f_8}{\partial T} \right| \leq k_{86}; \quad \frac{\partial f_8}{\partial H} = 0 \Rightarrow f_8(H) = k_{87}; \\ \frac{\partial f_8}{\partial E} = 0 \Rightarrow f_8(E) = k_{88}. \end{aligned} \quad (3.26)$$

Where k_{ij} ($1 \leq i,j \leq 8$) are all positive constants. Then from (3.19) to (3.26), each of the eight functions f_1, f_2, \dots, f_8 agree with the Lipschitz condition [18,39]. With respect to the eight arguments, then all eight functions are absolutely continuous.

4. Fractional order SIDARTHE model's optimal control strategy

In this area, the existence of the fractional order SIDARTHE model's optimal control is investigated and then the Hamiltonian of the optimal control problem is constructed in order to produce the optimal control necessary requirements.

Compute the optimal values of vaccination u_1 and treatment strategies u_2, u_3, u_4 that would maximize the Healed population phase (H) and minimize the determined infected phases (D, R, T) and susceptible (S) population phases. In addition, the charges of utilizing the vaccination and treatment methods are minimized. Then the optimal control problem of the following form is con-

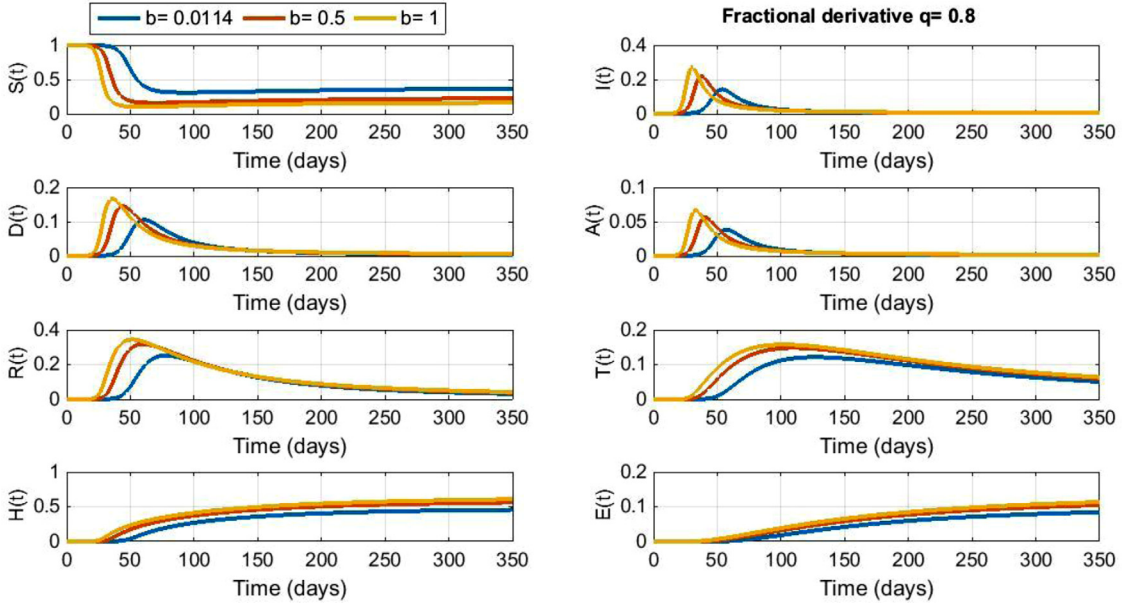


Fig. 17. The effect of changing the rate of infection (parameter b) on all population phases over the time where the fractional derivative order $q = 0.8$.

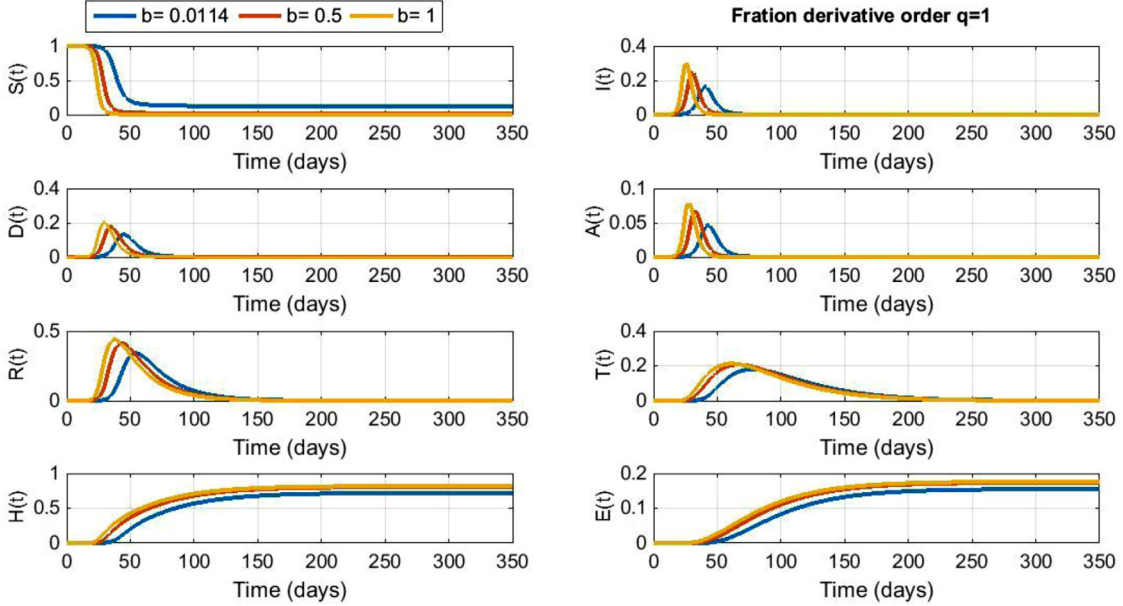


Fig. 18. The effect of changing the rate of infection (parameter b) on all population phases over the time where the fractional derivative order $q = 1$.

sidered (see for example [1,2,5,6,10,20,24,25,34,37,44–47].

$$\min_{(u_1, u_2, u_3, u_4) \in U} M(U(t)) = \begin{cases} S(T_f) + D(T_f) + R(T_f) + T(T_f) - H(T_f) \\ + \int_0^{T_f} \left((c_1 u_1^2 + c_2 u_2^2 + c_3 u_3^2 + c_4 u_4^2) dt \right. \\ \left. + S(t) + D(t) + R(t) + T(t) - H(t) \right) \end{cases} \quad (4.1)$$

That obeys the constraints

$$\begin{aligned} \Delta^q S(t) &= -(aS(t)I(t) + bS(t)D(t) + cS(t)A(t) + dS(t)R(t)) - u_1 S(t) = f_1, \\ \Delta^q I(t) &= aS(t)I(t) + bS(t)D(t) + cS(t)A(t) + dS(t)R(t) - (e + z + g)I(t) = f_2, \\ \Delta^q D(t) &= eI(t) - (h + r)D(t) - u_2 D(t) = f_3, \\ \Delta^q A(t) &= zI(t) - (\theta + m + k)A(t) = f_4, \\ \Delta^q R(t) &= hD(t) + \theta A(t) - (v + x)R(t) - u_3 R(t) = f_5, \\ \Delta^q T(t) &= mA(t) + vR(t) - (\sigma + \tau)T(t) - u_4 T(t) = f_6, \\ \Delta^q H(t) &= gI(t) + rD(t) + kA(t) + xR(t) + \sigma T(t) = f_7, \\ \Delta^q E(t) &= \tau T(t) = f_8. \end{aligned} \quad (4.2)$$

The control function $u_1(t)$ represents the vaccination strategy applied on the susceptible (S) population phase. The three control

functions $u_2(t), u_3(t), u_4(t)$ signify the treatment strategies applied on the determined infected population phases (D, R, T). All of the control functions are supposed to be $L^\infty(0, T_f)$ (T_f is the final time) functions belong to a collection of permissible controls:

$$U = \{(u_1, u_2, u_3, u_4) \in (L^8(0, T_f))^4 : u_{i \min} \leq u_i(t) \leq u_{i \max} \leq 1, i = 1, \dots, 4\}.$$

The four constants c_1, c_2, c_3 and c_4 are the cost correspond to utilizing each control function.

The uncontrolled system (put $u_i = 0$ in (4.2)). For certain initial conditions: $S(0) = S_0$, $I(0) = I_0$, $D(0) = D_0$, $A(0) = A_0$, $R(0) = R_0$, $T(0) = T_0$, $H(0) = H_0$, $E(0) = E_0$ such that their sum equal one, it is obvious that the final values of the state variables approach to an equilibrium: $S(T_f) = S_f$, $I(T_f) = 0$, $D(T_f) = 0$, $A(T_f) = 0$, $R(T_f) = 0$, $T(T_f) = 0$, $H(T_f) = H_f$, $E(T_f) = E_f$ where $S_f + H_f + E_f = 1$ which means that the phenomenon of epidemic is finished (see [21]). The possible equilibrium points of the system are given by $(S_f, 0, 0, 0, 0, H_f, E_f)$, where $S_f + H_f + E_f = 1$.

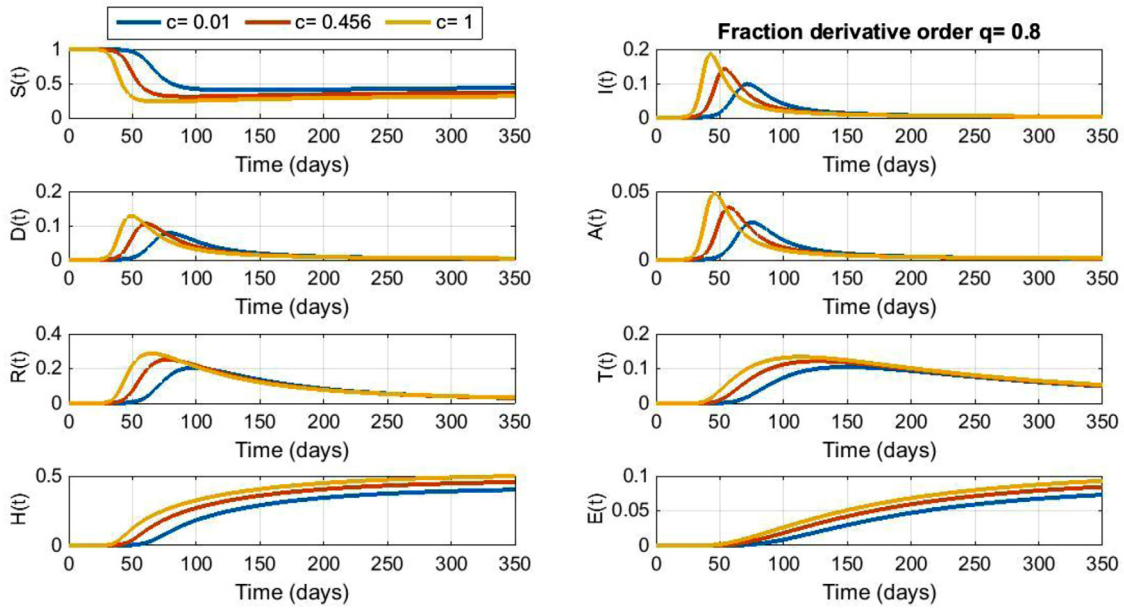


Fig. 19. The effect of changing the rate of infection (parameter c) on all population phases over the time where the fractional derivative order $q = 0.8$.

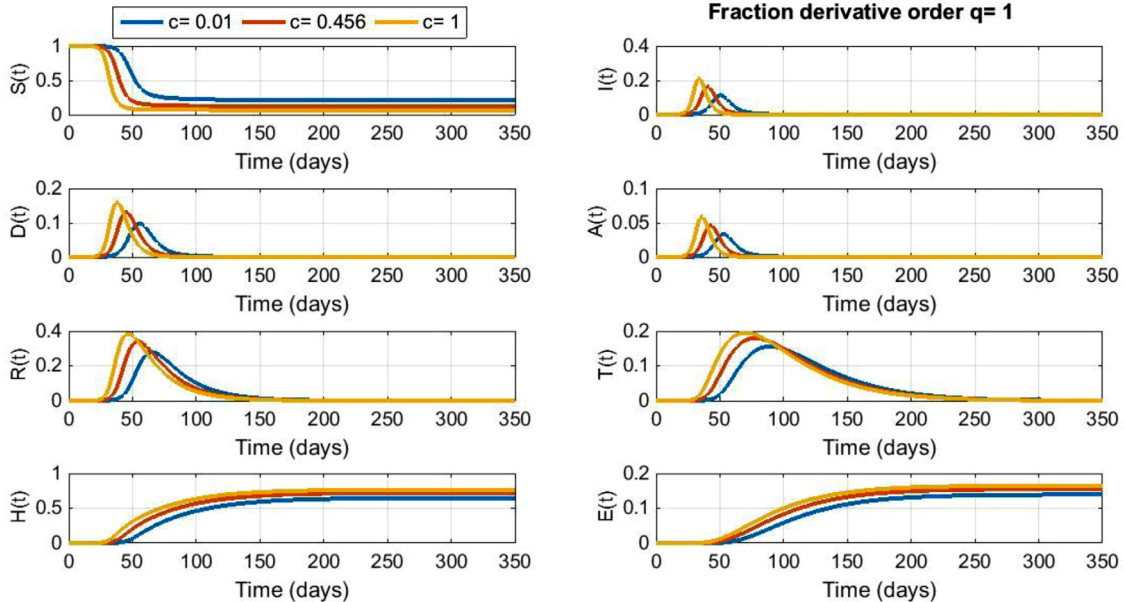


Fig. 20. The effect of changing the rate of infection (parameter c) on all population phases over the time where the fractional derivative order $q = 1$.

The incidence function of the system is:

$$f(S, I, D, A, R, T) = S(t)(al(t) + bD(t) + cA(t) + dR(t)) \quad (4.3)$$

In the following result, the existence of the optimal control is proved.

Theorem 4.1. For the problem of optimal control (4.1) with constraints (4.2). There exists an

optimal controls quadruple $(u_1, u_2, u_3, u_4) \in U$ and a related optimal states $(S^*, I^*, D^*, A^*, R^*, T^*, H^*, E^*)$ which minimize the objective function $M(U(t))$ over a collection of permissible controls U .

Proof. In order to prove the optimal control quadruple (u_1, u_2, u_3, u_4) existence, it is important to confirm the next assertions.

(I) The controls' collection and the related state variables is not empty.

- (II) The collection of permissible controls U is closed and convex.
- (III) The state model (4.2) is limited.
- (IV) The integration part of the objective function (4.1) $J_{SIDARTE}(u_1, u_2, u_3, u_4)$ is convex on the collection U .

The hessian matrix of integration part of the objective function (4.1) $J_{SIDARTE}(u_1, u_2, u_3, u_4)$ on U is given by:

$$\text{Hessian} = \begin{pmatrix} 2c_1 & 0 & 0 & 0 \\ 0 & 2c_2 & 0 & 0 \\ 0 & 0 & 2c_3 & 0 \\ 0 & 0 & 0 & 2c_4 \end{pmatrix},$$

$\text{SP}(\text{Hessian}) = \{2c_1, 2c_2, 2c_3, 2c_4\} \subset \mathbb{R}_+^*$, then the integration part of the objective function (4.1) $J_{SIDARTE}(u_1, u_2, u_3, u_4)$ is robustly convex in U .

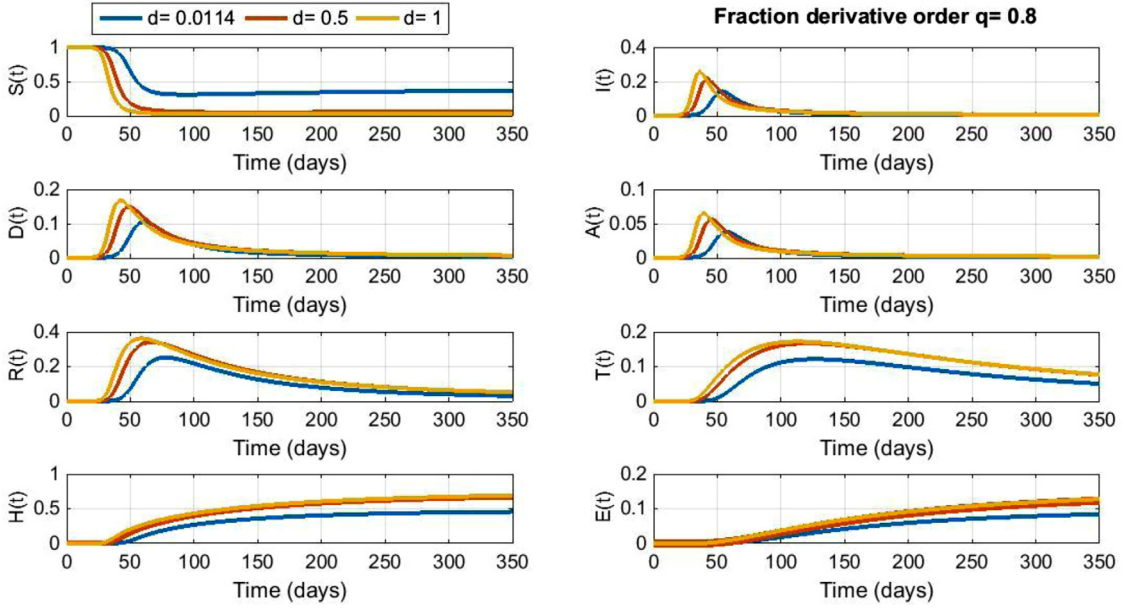


Fig. 21. The effect of changing the rate of infection (parameter d) on all population phases over the time where the fractional derivative order $q = 0.8$.

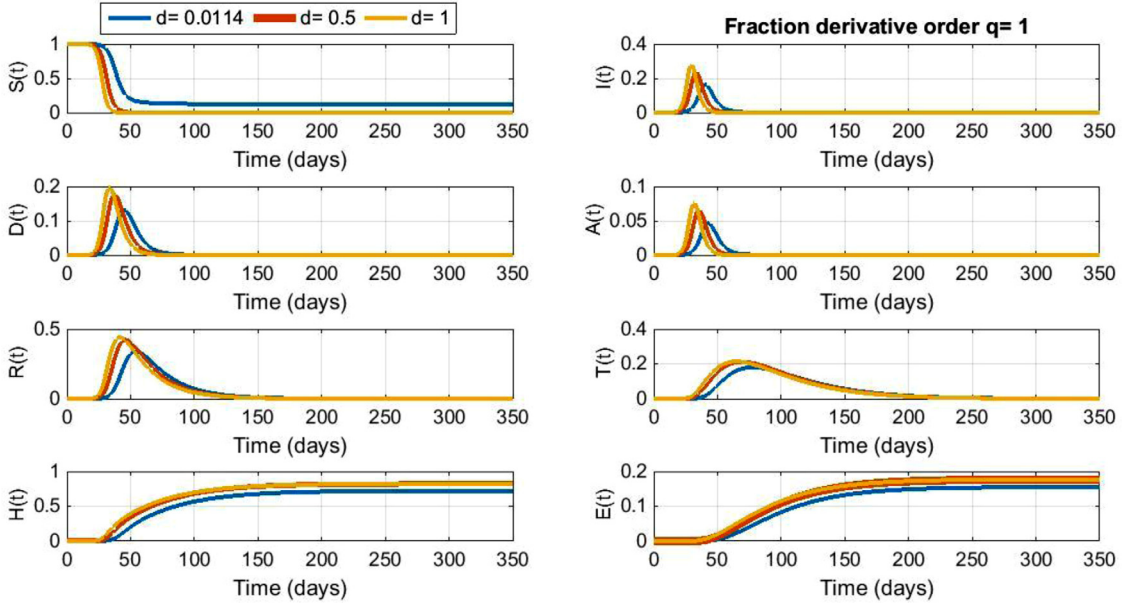


Fig. 22. The effect of changing the rate of infection (parameter d) on all population phases over the time where the fractional derivative order $q = 1$.

(I) There are constants $\beta_1 > 0$ and $\beta_2, \beta_3 > 1$ where $\int_{SIDARTHE} (u_1, u_2, u_3, u_4)$ satisfies:

$$\int_{SIDARTHE} (u_1, u_2, u_3, u_4) \geq \beta_1 |(u_1, u_2, u_3, u_4)|^{\beta_3} - \beta_2.$$

$$\begin{aligned} \int_{SIDARTHE} (u_1, u_2, u_3, u_4) &= c_1 u_1^2(t) + c_2 u_2^2(t) + c_3 u_3^2(t) \\ &\quad + c_4 u_4^2(t) + S(t) + D(t) + R(t) + T(t) - H(t) \\ &\geq \min(c_1, c_2, c_3, c_4) (u_1^2(t) + u_2^2(t) + u_3^2(t) + u_4^2(t)) - H(t) \end{aligned}$$

Since $S + I + D + A + R + T + H + E = 1$ then $H(t)$ is bounded. That is mean there exist two constants H_1 and H_2 such that $H_1 \leq H(t) \leq H_2, \forall t$

Assume that $\beta_1 = \min(c_1, c_2, c_3, c_4)$ and $\beta_2 = H_2$, then we have:

$$\int_{SIDARTHE} (u_1, u_2, u_3, u_4) \geq \beta_1 \|(u_1, u_2, u_3, u_4)\|^2 - \beta_2.$$

4.1. Implementation of optimal control

This subsection records the needed conditions for the optimal control to be exist. The necessary conditions are computed here via constructing the Hamiltonian (Φ) and satisfying the maximum basis of Pontryagin [5]. Let us denote by $X = [S(t), I(t), D(t), A(t), R(t), T(t), H(t), E(t)]^T$ the system states, by $u(t) = [u_1, u_2, u_3, u_4]^T$ the vector of control functions, by $\lambda(t) = [\lambda_1, \lambda_2, \lambda_3, \lambda_4, \lambda_5, \lambda_6, \lambda_7, \lambda_8]$ the Lagrange multipliers and by $\int_{SIDARTHE} (X(t), u(t))$ the integration part of the objective function (3.1).

$$\begin{aligned} \text{Then the Hamiltonian } \Phi &= \Phi(X(t), \lambda(t), u(t)) = \int_{SIDARTHE} (X(t), u(t)) + \lambda^T \Delta^q X(t), \\ \Phi &= c_1 u_1^2 + c_2 u_2^2 + c_3 u_3^2 + c_4 u_4^2 + S + D + R + T - H + \sum_{i=1}^8 \lambda_i f_i \end{aligned} \quad (4.4)$$

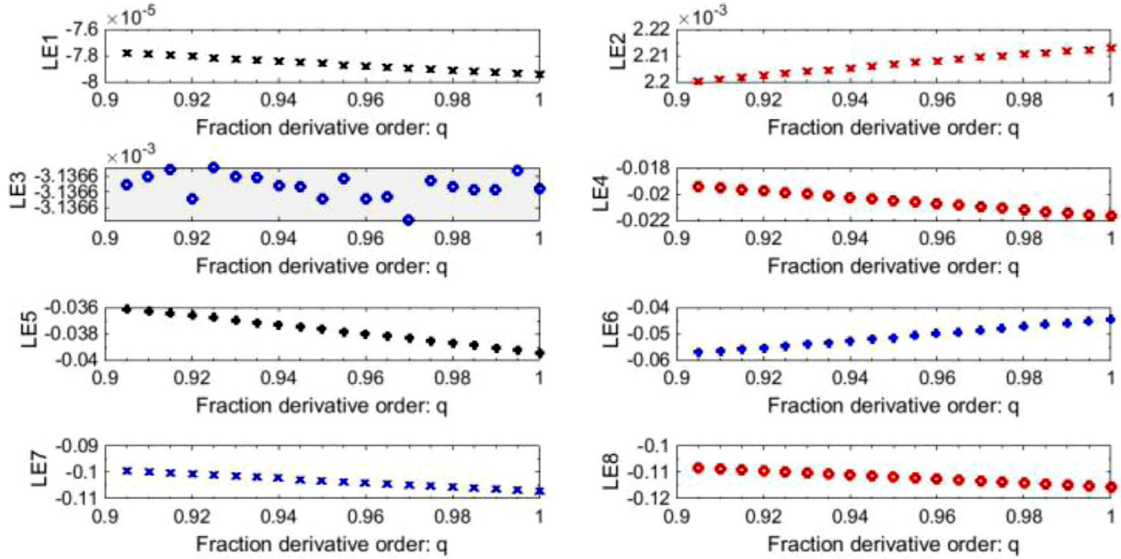


Fig. 23. The effect of changing the fractional derivative order q on the system eight Lyapunov exponents (LE1, LE2, ..., LE8).

Assume that the characterization functional is formed as:

$$\Gamma_{[0, T_f]}(t) = \begin{cases} 1, & \text{if } t \in [0, T_f], \\ 0, & \text{otherwise.} \end{cases} \quad (4.5)$$

Assume that $u^*(t) = [u_1^*, u_2^*, u_3^*, u_4^*]^T$ is the optimal controls and $X^* = [S^*(t), I^*(t), D^*(t), A^*(t), R^*(t), T^*(t), H^*(t), E^*(t)]^T$ be the related optimal population phases fractions. Consequently, there exists $\lambda(t) \in \mathbb{R}^8$ such that the necessary conditions for the optimal control to be exist are produced by (see for example [5]):

$$\begin{aligned} \frac{\partial \Phi}{\partial u}(t) &= 0, \\ \Delta^q X(t) &= \frac{\partial \Phi}{\partial \lambda}, \\ \Delta^q \lambda &= -\frac{\partial \Phi}{\partial X} \end{aligned} \quad (4.6)$$

From (4.4) and (4.6), the optimization constraints can be found as:

$$\begin{aligned} \frac{\partial \Phi}{\partial u_1}(t) &= 2c_1 u_1^* - \lambda_1 S = 0, \\ \frac{\partial \Phi}{\partial u_2}(t) &= 2c_2 u_2^* - \lambda_3 D = 0, \\ \frac{\partial \Phi}{\partial u_3}(t) &= 2c_3 u_3^* - \lambda_5 R = 0, \\ \frac{\partial \Phi}{\partial u_4}(t) &= 2c_4 u_4^* - \lambda_6 T = 0, \end{aligned} \quad (4.7)$$

From (4.7), we can find that

$$\begin{aligned} u_1^* &= \min \left\{ u_1 \max, \max \left\{ 0, \frac{\lambda_1(t)S(t)}{2c_1} \right\} \right\}, \\ u_2^* &= \min \left\{ u_2 \max, \max \left\{ 0, \frac{\lambda_3(t)D(t)}{2c_2} \right\} \right\}, \\ u_3^* &= \min \left\{ u_3 \max, \max \left\{ 0, \frac{\lambda_5(t)R(t)}{2c_3} \right\} \right\}, \\ u_4^* &= \min \left\{ u_4 \max, \max \left\{ 0, \frac{\lambda_6(t)T(t)}{2c_4} \right\} \right\}. \end{aligned} \quad (4.8)$$

From the state variables system given in (4.2), the co-state conditions are:

$$\frac{d\lambda_i}{dt}(t) = -\frac{\partial \Phi}{\partial X_i}(t), \quad i = 1, 2, \dots, 8. \quad (4.9)$$

Which can be simplified to produce the following co-state system:

$$\begin{aligned} \Delta^q \lambda_1(t) &= -\frac{\partial \Phi}{\partial S}(t) = -1 + (al + bD + cA + dR)(\lambda_1(t) + \lambda_2(t)) \\ &\quad + u_1 \lambda_1(t); \\ \Delta^q \lambda_2(t) &= -\frac{\partial \Phi}{\partial I}(t) = aS(\lambda_1(t) - \lambda_2(t)) + (e + z + g)\lambda_2(t) \\ &\quad - e\lambda_3(t) - z\lambda_4(t) - g\lambda_7(t); \end{aligned}$$

$$\begin{aligned} \Delta^q \lambda_3(t) &= -\frac{\partial \Phi}{\partial D}(t) = -1 + bS\lambda_1(t) - bS\lambda_2(t) \\ &\quad + (h + r + u_2)\lambda_3(t) - h\lambda_5(t) - r\lambda_7(t); \\ \Delta^q \lambda_4(t) &= -\frac{\partial \Phi}{\partial A}(t) = cS\lambda_1(t) - cS\lambda_2(t) + (\theta + m + k)\lambda_4(t) \\ &\quad - \theta\lambda_5(t) - m\lambda_6(t) - k\lambda_7(t); \\ \Delta^q \lambda_5(t) &= -\frac{\partial \Phi}{\partial R}(t) = -1 + dS\lambda_1(t) - dS\lambda_2(t) + (v + x + u_3)\lambda_5(t) \\ &\quad - v\lambda_6(t) - x\lambda_7(t); \\ \Delta^q \lambda_6(t) &= -\frac{\partial \Phi}{\partial T}(t) = -1 + (\sigma + \tau + u_4)\lambda_6(t) - \sigma\lambda_7(t) - \tau\lambda_8(t); \\ \Delta^q \lambda_7(t) &= -\frac{\partial \Phi}{\partial H}(t) = 1; \\ \Delta^q \lambda_8(t) &= -\frac{\partial \Phi}{\partial E}(t) = 0; \end{aligned} \quad (4.10)$$

The transversality conditions leads to $\lambda_i(T_f) = \begin{cases} -1, & i = 7 \\ 1, & \text{otherwise.} \end{cases}$

Notation 4. .2. From the above discussion, it is obvious that

- I The Hamiltonian functional Φ is robustly convex in the variables of control.
- II The state Eqs. (4.2) and co-state Eqs. (4.10) are Lipschitz continuous.
- III The collection of permissible controls U is convex.

The effect of applying the different control strategies will be simulated numerically in Section 6.

5. Fractional order numerical simulation of the SIDARTHE uncontrolled model

In this fifth section, we solve the fractional order SIDARTHE model numerically utilizing the predictor-corrector PECE method of Adams-Bashforth-Moulton type described in details in [15,19].

The parameters' values used for the numerical simulation are estimated from the Italian real life statistics published in [21] where: $a = 0.57$; $b = 0.0114$; $c = 0.456$; $d = 0.0114$; $e = 0.171$; $\theta = 0.3705$; $z = 0.1254$; $h = 0.1254$; $m = 0.0171$; $v = 0.0274$; $\tau = 0.01$; $g = 0.0342$; $r = 0.0342$; $k = 0.0171$; $x = 0.0171$; $\sigma = 0.0171$.

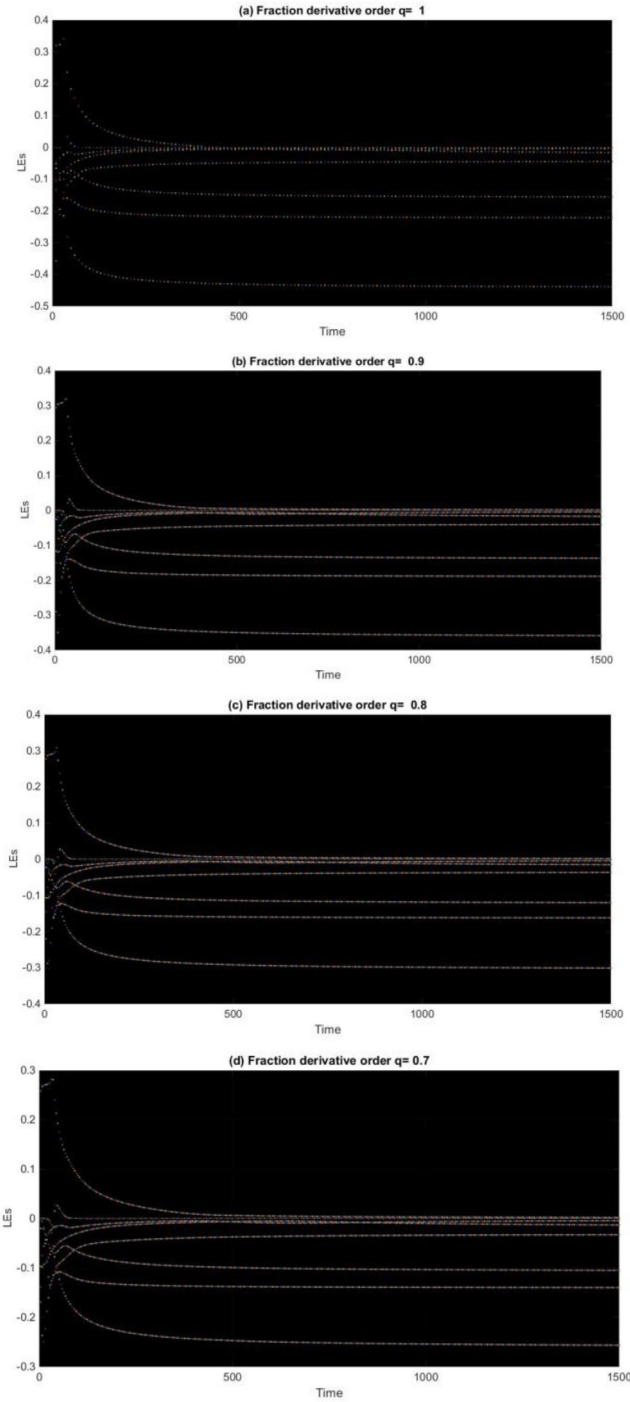


Fig. 24. Lyapunov Exponents of the model over time: (a) $q = 1$ (b) $q = 0.9$ (c) $q = 0.8$ (d) $q = 0.7$.

The total population are taken 100 Million and the initial values of the different population phases after normalization are (let N be the total population):

$$I(0) = \frac{200}{N}; D(0) = \frac{20}{N}; A(0) = \frac{1}{N};$$

$$R(0) = \frac{2}{N}; T(0) = 0; H(0) = 0; E(0) = 0;$$

$$S(0) = 1 - I(0) - D(0) - A(0) - R(0) - T(0) - H(0) - E(0);$$

$$X(0) = [S(0), I(0), D(0), A(0), R(0), T(0), H(0), E(0)];$$

In the following, we display the results of the numerical simulation of the uncontrolled SIDARTHE model. Fig. 2 displays the time history of susceptible cases ($S(t)$) and infected, symptomless, undetermined cases ($I(t)$) with different fractional derivative order (q): (a) time history of $S(t)$ with $q = 0.7, 0.8, 0.9, 1$; (b) time history of $I(t)$ with $q = 0.7, 0.8, 0.9, 1$. Fig. 3 displays the time history of diagnosed, infected, symptomless, determined cases ($D(t)$) and ailing, infected, symptomatic, undetermined cases ($A(t)$) with different fractional derivative order (q): (a) time history of $D(t)$ with $q = 0.7, 0.8, 0.9, 1$; (b) time history of $A(t)$ with $q = 0.7, 0.8, 0.9, 1$. Fig. 4 displays the time history of recognized, infected, symptomatic, determined cases ($R(t)$) and threatened, infected, symptomatic, determined cases ($T(t)$) with different fractional derivative order (q): (a) time history of $R(t)$ with $q = 0.7, 0.8, 0.9, 1$; (b) time history of $T(t)$ with $q = 0.7, 0.8, 0.9, 1$. Fig. 5 displays the time history of the total infected cases: $TI(t) = I(t) + D(t) + A(t) + R(t) + T(t)$, with different fractional derivative order $q = 0.7, 0.8, 0.9, 1$. Fig. 6 displays the time history of healed cases ($H(t)$) and died out (Extinct) cases ($E(t)$) with different fractional derivative order (q): (a) time history of $R(t)$ with $q = 0.7, 0.8, 0.9, 1$; (b) time history of $T(t)$ with $q = 0.7, 0.8, 0.9, 1$. Fig. 7 displays the three-dimensions plot of the state variables: diagnosed, infected, symptomless, determined cases ($D(t)$), infected, symptomless, undetermined cases ($I(t)$) and susceptible cases ($S(t)$) with different fractional derivative order $q = 0.7, 0.8, 0.9, 1$. Fig. 8 displays the three-dimensions plot of the state variables: healed cases ($H(t)$), total infected ($TI(t) = I(t) + D(t) + A(t) + R(t) + T(t)$) and susceptible cases ($S(t)$) with different fractional derivative order $q = 0.7, 0.8, 0.9, 1$. Fig. 9 displays the phase plane of state variables: total infected ($TI(t) = I(t) + D(t) + A(t) + R(t) + T(t)$) and susceptible cases ($S(t)$) with different fractional derivative order $q = 0.7, 0.8, 0.9, 1$. Fig. 10 displays the phase plane of state variables: total infected $TI(t) = I(t) + D(t) + A(t) + R(t) + T(t)$ and healed cases ($H(t)$) with different fractional derivative order $q = 0.7, 0.8, 0.9, 1$.

From the results and the figures mentioned here, we can state that decreasing the fractional derivative order q decreases the number of each population phase (except Susceptible population fraction as expected) and flatten the curves also delays reaching the maximum in each population phase.

5.1. Parameters impact on different population phases

In this subsection, we show the effect of changing certain system parameters on different population phases at day 60 with various fractional derivative order. Fig. 11 displays the effect of changing the rate of infection (parameter a) on different population phases at day 60 with different fractional derivative order $q = 0.7, 0.8, 0.9, 1$. Fig. 12 displays the effect of changing the rate of infection (parameter b) on different population phases at day 60 with different fractional derivative order $q = 0.7, 0.8, 0.9, 1$. Figs. 13, 14, 15, 16 display the effect of changing the rate of infection (parameter a) on all population phases over time where the fractional derivative order $q = 0.7, 0.8, 0.9, 1$, respectively. Figs. 17, 18 display the effect of changing the rate of infection (parameter b) on all population phases over the time where the fractional derivative order $q = 0.8$ and 1, respectively. Figs. 19, 20 display the effect of changing the rate of infection (parameter c) on all population phases over the time where the fractional derivative order

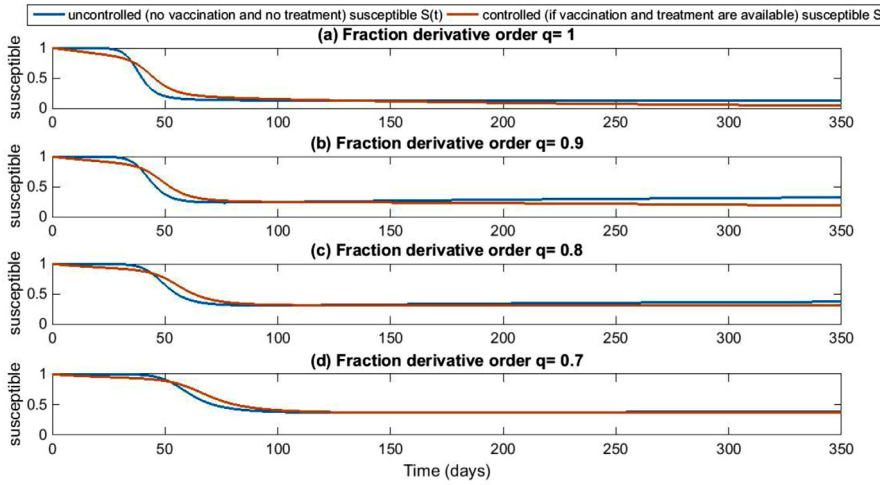


Fig. 25. Time history of Susceptible cases in uncontrolled (no vaccination and no treatment) case and with control (vaccination and treatment are available) with different fractional derivative order: (a) $q = 0.1$, (b) $q = 0.9$, (c) $q = 0.8$, (c) $q = 0.7$.

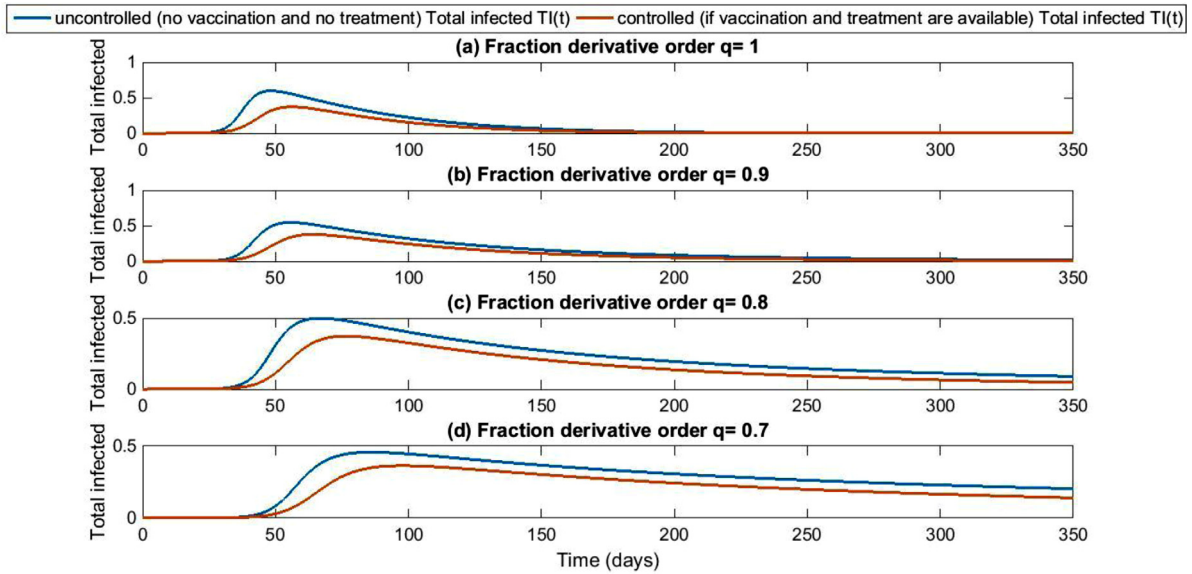


Fig. 26. Time history of total infected cases in uncontrolled (no vaccination and no treatment) case and with control (vaccination and treatment are available) with different fractional derivative order: (a) $q = 0.1$, (b) $q = 0.9$, (c) $q = 0.8$, (c) $q = 0.7$.

$q = 0.8$ and 1, respectively. Fig. 21,22 display the effect of changing the rate of infection (parameter d) on all population phases over the time where the fraction derivative order $q = 0.8$ and 1, respectively.

From the results shown in all figures mentioned in the previous paragraph and plotted in the current subsection, we can state that decreasing the fractional derivative order q decreases the number of infected cases and delays the time of reaching the maximum number in each population phase. Decreasing the fractional derivative order q makes the curves of all population phases more flat. In addition, decreasing the infection rates a, b, c and d decreases the number of cases in all population phases except the susceptible as expected.

5.2. Lyapunov exponents of the fractional order SIDARTHE model

The mean rate of separation or contraction of tiny phase-space disturbances of a dynamical system beginning from near starting points is metered by the Lyapunov exponents (LEs) [55],[59]. Thus,

they can be utilized to study the stability of dynamical systems and to examine sensitive reliance on starting conditions, that implies, the presence of hidden chaotic dynamics. It is important to check the epidemic transition models if it is chaotic or not via calculating LEs. Corresponding techniques for the LEs calculation and their distinction are studied, e.g., in [35,36].

The studied system represented by equations: (3.1) – (3.8) is stable [21]. Here, we confirm its stability for different values of fractional derivative order via plotting the relationship between the fraction derivative order and the eight Lyapunov exponents of the system. Fig. 23 shows that all system eight Lyapunov exponents are negative with different fraction derivative order as time approaches infinity (here, time is taken 1500). Fig. 24 shows the dynamics of the system eight Lyapunov exponents with time. In Fig. 24-(a) to 24-(d) with different fraction derivative order, the system eight Lyapunov exponents approaches negative end which confirm the system stability with different fractional derivative orders. For more details about Lyapunov exponents see [55]. Here,

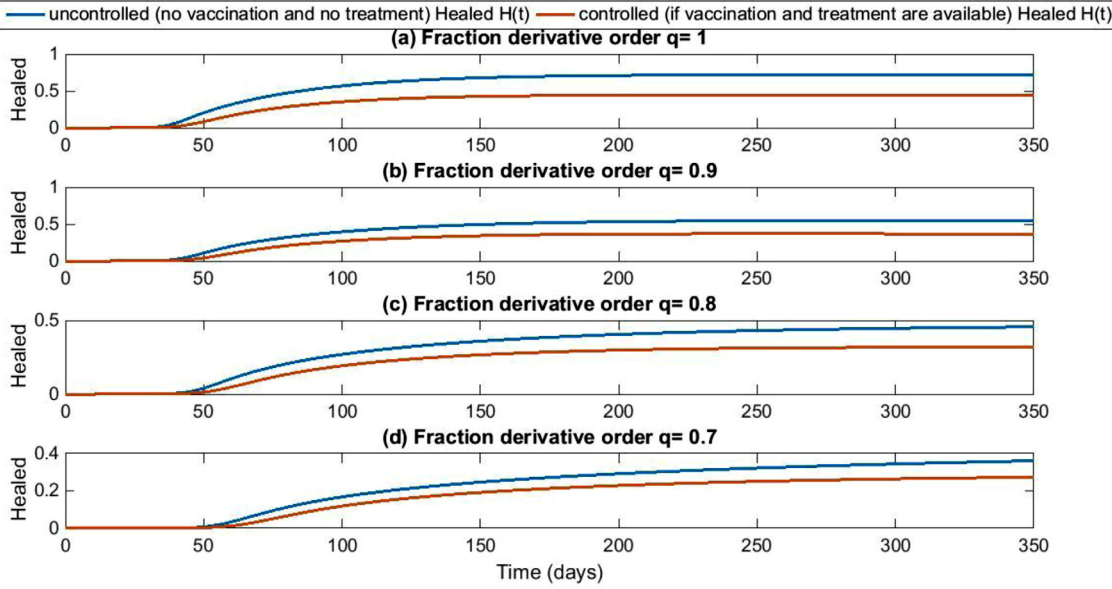


Fig. 27. Time history of Healed cases in uncontrolled (no vaccination and no treatment) case and with control (vaccination and treatment are available) with different fractional derivative order: (a) $q = 0.1$, (b) $q = 0.9$, (c) $q = 0.8$, (d) $q = 0.7$.

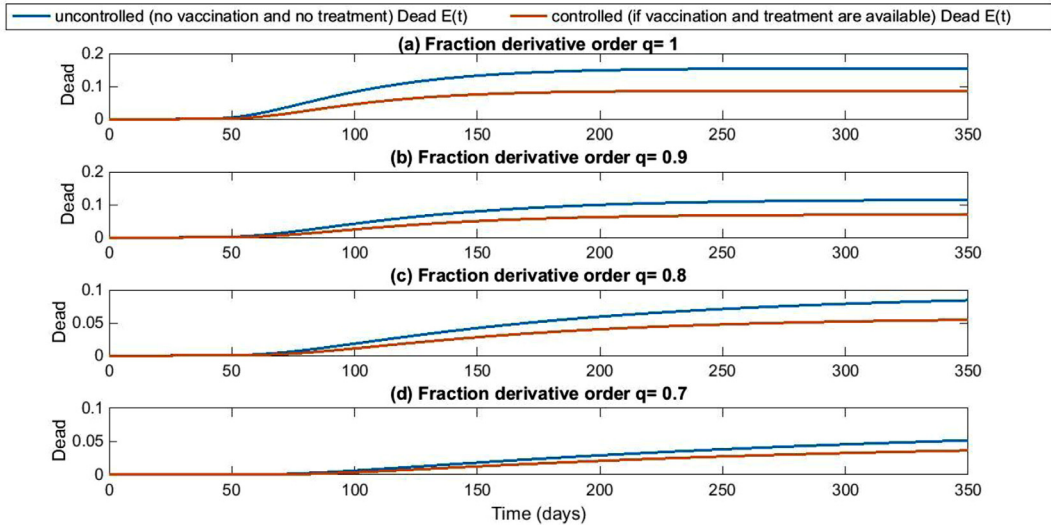


Fig. 28. Time history of Dead cases in uncontrolled (no vaccination and no treatment) case and with control (vaccination and treatment are available) with different fractional derivative order: (a) $q = 0.1$, (b) $q = 0.9$, (c) $q = 0.8$, (d) $q = 0.7$.

we use the method in [13] for calculating the fractional order Lyapunov exponents.

6. Numerical simulation of the controlled system

In this section, we show numerically, the effect of applying the four control strategies studied in Section 3. Fig. 25 shows the time history of Susceptible cases in uncontrolled (no vaccination and no treatment) case and with control (vaccination and treatment

are available) with different fractional derivative order: (a) $q = 0.1$, (b) $q = 0.9$, (c) $q = 0.8$, (c) $q = 0.7$. Fig. 26. Shows the time history of total infected cases in uncontrolled (no vaccination and no treatment) case and with control (vaccination and treatment are available) with different fractional derivative order: (a) $q = 0.1$, (b) $q = 0.9$, (c) $q = 0.8$, (c) $q = 0.7$. Fig. 27 shows the time history of Healed cases in uncontrolled (no vaccination and no treatment) case and with control (vaccination and treatment are available) with different fractional derivative order: (a) $q = 0.1$, (b) $q = 0.9$,

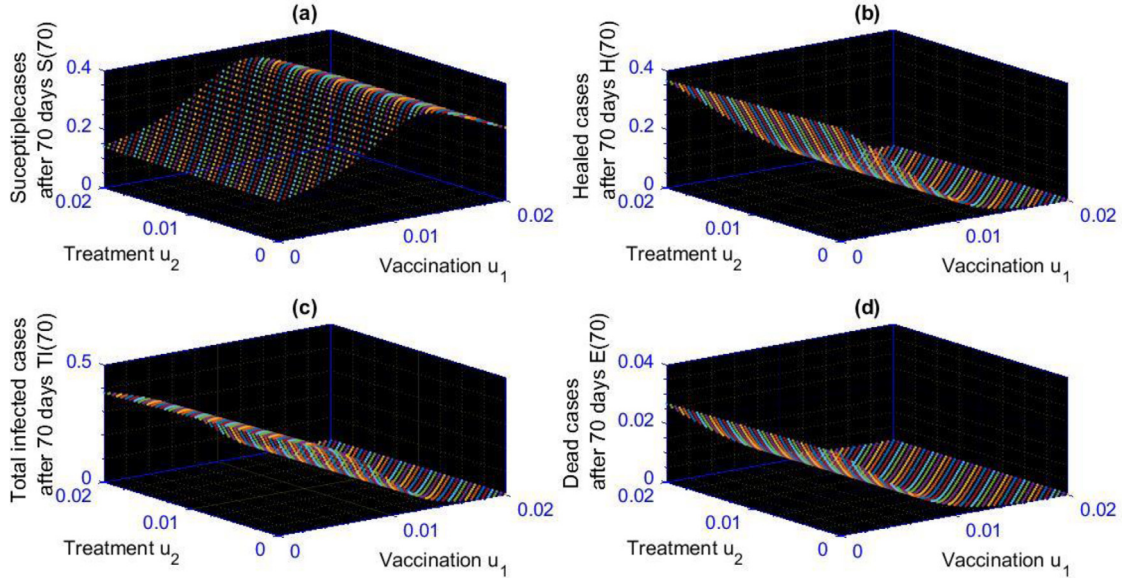


Fig. 29. The effect of the control strategies: u_1 (vaccination) and u_2 (treatment of the Diagnosed population phase D) on the different population phases at day 70 with fractional derivative order $q = 1$.

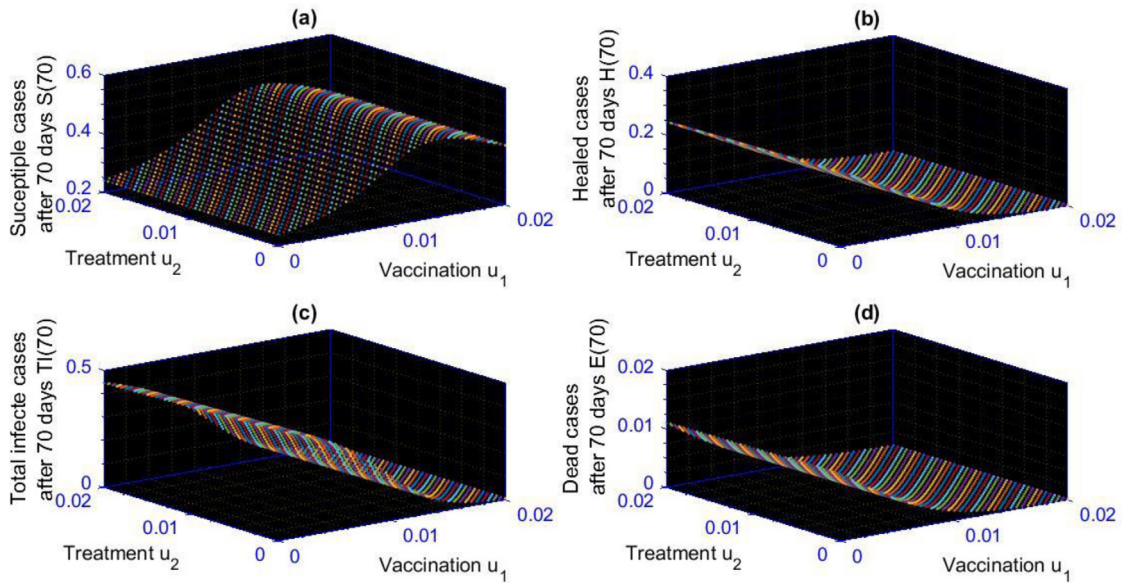


Fig. 30. The effect of the control strategies: u_1 (vaccination) and u_2 (treatment of the Diagnosed population phase D) on the different population phases at day 70 with fractional derivative order $q = 0.9$.

(c) $q = 0.8$, (c) $q = 0.7$. Fig. 28 shows the time history of Dead cases in uncontrolled (no vaccination and no treatment) case and with control (vaccination and treatment are available) with different fractional derivative order: (a) $q = 0.1$, (b) $q = 0.9$, (c) $q = 0.8$, (c) $q = 0.7$. Fig. 29 shows the effect of the control strategies: u_1 (vaccination) and u_2 (treatment of the Diagnosed population phase D) on the different population phases at day 70 with fractional derivative order $q = 1$. Fig. 30 shows the effect of the control strategies:

u_1 (vaccination) and u_2 (treatment of the Diagnosed population phase D) on the different population phases at day 70 with fractional derivative order $q = 0.9$. Fig. 31 shows the effect of the control strategies: u_3 (treatment of the Recognized population phase R) and u_4 (treatment of the Threatened population phase T) on the different population phases at day 70 with fraction derivative order $q = 1$. Fig. 32 shows the effect of the control strategies: u_3 (treatment of the Recognized population phase R) and u_4 (treat-

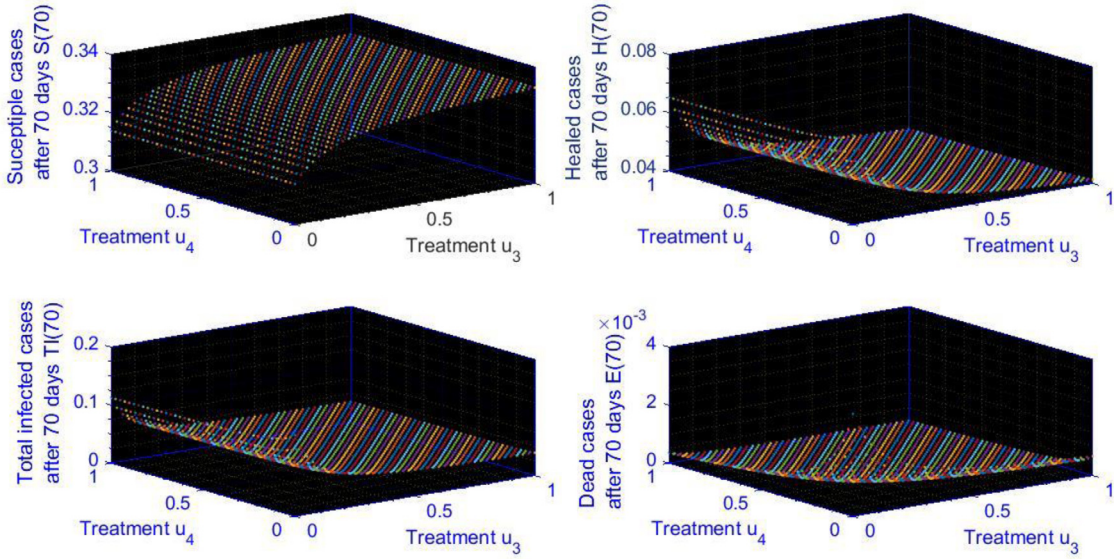


Fig. 31. The effect of the control strategies: u_3 (treatment of the Recognized population phase R) and u_4 (treatment of the Threatened population phase T) on the different population phases at day 70 with fractional derivative order $q = 1$.

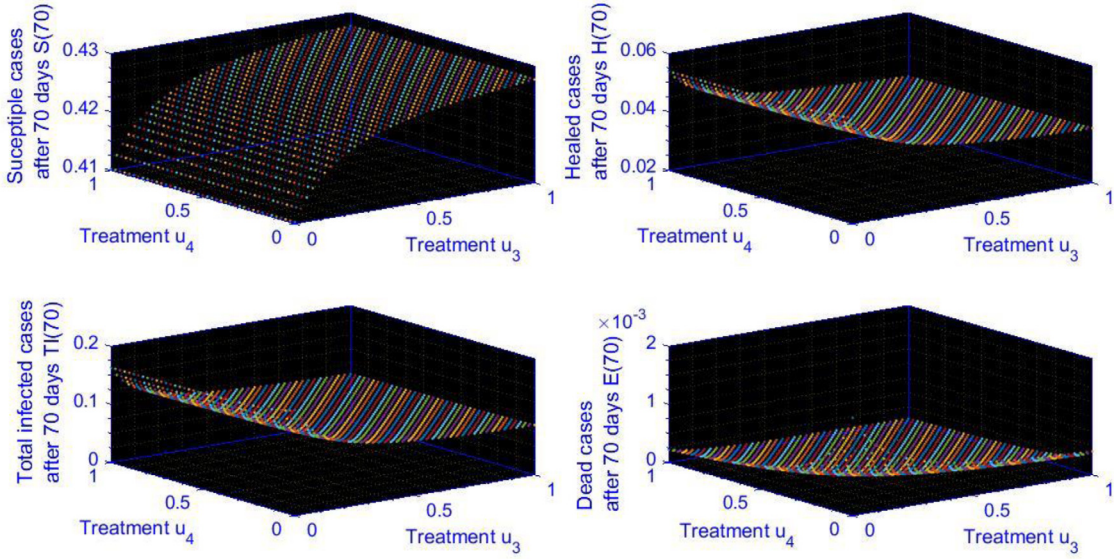


Fig. 32. The effect of the control strategies: u_3 (treatment of the Recognized population phase R) and u_4 (treatment of the Threatened population phase T) on the different population phases at day 70 with fractional derivative order $q = 0.9$.

ment of the Threatened population phase T) on the different population phases at day 70 with fractional derivative order $q = 0.9$. From all of these simulations, we can claim that the availability of the vaccination and (or) treatment has a great effect of the spread of the COVID-19 pandemic and on the cases on each population phase.

7. Conclusion

This research has been carried out to the analysis of an eight dimension fractional order SIDARTHE COVID-19 mathematical model. In this 8-D COVID-19 mathematical model, the infected population fraction is partitioned into five different population fractions: I, D, A, R and T . It is the first time to study such model with fractional order. The existence of stable solution of the fractional order

SIDARTHE model is proved. The fractional order necessary conditions for a four optimal control strategies are implemented. In addition, the system dynamics displayed via the fraction order numerical solver by MATLAB software with different fractional orders and the effects of changing the infection rates parameters are presented in this manuscript with different fractional orders. The effects of changing the fractional order on the system Lyapunov exponent are also displayed. The dynamics of the system are presented before and after control. From our study, we can state that decreasing the fractional derivative order decreases the number of cases in all population fraction phases and delays the maximum plus changing the value of the fractional derivative order has no effect on the stability of the system since its all Lyapunov exponents still negative. The proposed fractional order COVID-19 SIDARTHE model predicts the evolution of COVID-19 epidemic and try to help

in understanding the impact of different plans to limit the diffusion of this epidemic with different values of the fractional order. Our results confirm the importance of decreasing the infection rates. Decreasing the infection rates include taking various actions like insure the social distance, closing the airports, closing all teaching authorities, random testing the asymptomatic cases and contact tracing. The author hope that COVID-19 study using the proposed model continues. And via utilizing the real data the optimum fractional order can be estimated.

Declaration of Competing Interest

No competing of interest.

Funding

This research did not receive any specific grant from funding agencies in the public, commercial, or not-for-profit sectors.

References

- [1] Abta A, Laarabi H, Alaoui HT. The hopf bifurcation analysis and optimal Control of a delayed SIR epidemic model. *Int. J. Anal.* 2014;2014:1–10.
- [2] Aldila D, Gotz T, Soewono E. An optimal Control problem arising from a dengue disease transmission model. *Math. Biosci.* 2013;242(1):9–16.
- [3] Anastassopoulou C, Russo L, Tsakris A, Siettos C. Data-based analysis, modelling and forecasting of the COVID-19 outbreak. *PLoS ONE* 2020;15:e0230405.
- [4] Anderson RM, May RM. Infectious diseases of humans. Oxford Univ. Press; 1991.
- [5] Barro M, Abdoumame Guiro, Dramane Ouedraogo. Optimal control of a SIR epidemic model with general incidence function and a time delays. *CUBO A Mathematical Journal* 2018;20(02):53–66.
- [6] Ball FG, Knock ESPD. O'Neil Control of emerging infectious diseases using responsive imperfect vaccination and isolation. *Math. Biosci.* 2008;216(1):100–13.
- [7] Becker N. The use of epidemic models. *Biometrics* 1978;35:295–305.2.
- [8] Brauer F, Castillo-Chavez C. Mathematical models in population biology and epidemiology. Springer; 2012. 2nd edn.
- [9] Casella F. Can the COVID-19 epidemic be managed on the basis of daily data? Preprint at <https://arxiv.org/abs/2003.06967>. (2020).
- [10] Castilho C. Optimal Control of an epidemic through educational campaigns. *Electron. J. Differ. Equ.* 2006;2006:1–11.
- [11] Chiyaka C, Garira W, Dube S. Transmission model of endemic human malaria in a partially immune population. *Math. Comput. Model.* 2007;46:806–22.
- [12] Sebastián Contreras, H Andrés, Villavicencio DavidMedina-Ortíz, Juan PabloBiron-Lattes, Álvaro Olivera-Nappa. A multi-group SEIRA model for the spread of COVID-19 among heterogeneous populations, *Chaos, Solitons & Fractals*. Available online 2020;25:109925. May <https://doi.org/10.1016/j.chaos.2020.109925>.
- [13] Marius-F Danca, Nikolay Kuznetsov. Matlab Code for Lyapunov Exponents of Fractional-Order Systems. *International Journal of Bifurcation and Chaos* 2018;28:1850067. 2018No. 5 <https://doi.org/10.1142/S0218127418500670>.
- [14] Diekmann O, Heesterbeek JAP. Mathematical epidemiology of infectious diseases: model building, Analysis and Interpretation; 2000. Wiley.
- [15] Diethelm K, Freed AD. The FracPECE subroutine for the numerical solution of differential equations of fractional order. In: Heinzel S, Plesser T, editors. Research and scientific computing 1998. society for scientific data processing, 1999. Göttingen; 1999. p. 57–71.
- [16] Dietz K. The first epidemic model: a historical note on P.D. En'ko. *Aust. J. Stat.* 1988;30A:56–65.
- [17] El-Dessoky MM, Khan MA. Modeling and analysis of the polluted lakes system with various fractional approaches. *Chaos, Solitons & Fractals* 2020;134:1–14. <https://doi.org/10.1016/j.chaos.2020.109720>.
- [18] El-Shahed M, Alsaedi A. The fractional SIRC model and influenza A. *Mathematical Problems in Engineering* 2011;2011:1–9.
- [19] Garrappa R. On linear stability of predictor-corrector algorithms for fractional differential equations. *Internat. J. Comput. Math.* 2010;87(10):2281–90.
- [20] Gaff H, Schaefer E. Optimal control applied to vaccination and treatment strategies for various epidemiological models. *Math. Biosci. Eng.* 2009;6(3):469–92.
- [21] Giulia Giordano, Franco Blanchini, Raffaele Bruno, Patrizio Colaneri, Alessandro Di Filippo, Angela Di Matteo, et al. Modelling the COVID-19 epidemic and implementation of population-wide interventions in Italy. *Nat. Med.* April 2020;22. <https://doi.org/10.1038/s41591-020-0883-7>.
- [22] Guan W-J, et al. Clinical characteristics of coronavirus disease 2019 in China. *N. Engl. J. Med.* 2020. <https://doi.org/10.1056/NEJMoa2002032>.
- [23] Gumel AB, et al. Modelling strategies for controlling SARS outbreaks. *Proc. R. Soc. B Biol. Sci.* 2004. <https://doi.org/10.1098/rspb.2004.2800>.
- [24] Youssi Hattaf N. Optimal Control of a delayed HIV infection model with immune response using an efficient numerical method. *Int. Sch. Res. Netw.* 2012;2012:1–7.
- [25] Hellewell J, et al. Feasibility of controlling COVID-19 outbreaks by isolation of cases and contacts. *Lancet Global Health* 2020;8:488–96.
- [26] Hethcote HW. The mathematics of infectious diseases. *SIAM Rev* 2000;42:599–653.
- [27] Hethcote HW, Driessche P. Some epidemiological models with nonlinear incidence. *J.Math. Biol.* 1991;29:271–87.
- [28] Hethcote HW. The mathematics of infectious. *SIAM Rev* 2000;42:599–653.
- [29] Kaddar A. On the dynamics of a delayed SIR epidemic model with a modified saturated incidence rate. *Electron. J. Differ. Equ.* 2009;13:1–7.
- [30] Khader MM, Sweilam NH, Mahdy AMS, Abdel Moniem NK. Numerical simulation for the fractional SIRC model and Influenza A. *Appl. Math. Inf. Sci.* 2014;8(3):1–8.
- [31] Khan MA, Atangana A. Modeling the dynamics of novel coronavirus (2019-nCoV) with fractional derivative. *Alexandria Engineering Journal* 2020;1–11. <https://doi.org/10.1016/j.aej.2020.02.033>.
- [32] Khan MA, Ismail M, Ullah S, Farhan M. Fractional order SIR model with generalized incidence rate. *AIMS Mathematics* 1856;5(3):1856–80.
- [33] Kermack WO, McKendrick AG. A contribution to the mathematical theory of epidemics. *Proc. R. Soc. Lond.* 1927;115:700–21.
- [34] Kucharski AJ, et al. Early dynamics of transmission and control of COVID-19: a mathematical modelling study. *Lancet Global Health* 2020;3099(20):30144. [https://doi.org/10.1016/S1473-3099\(20\)30144-4](https://doi.org/10.1016/S1473-3099(20)30144-4).
- [35] Kuznetsov N, Alexeeva T, Leonov G. Invariance of Lyapunov exponents and Lyapunov dimension for regular and irregular linearizations. *Nonlinear Dyn* 2016;85:195–201. doi: <https://doi.org/10.1007/s11071-016-2678-z>.
- [36] Kuznetsov N, Leonov G, Mokaev T, Prasad A, Shrimali M. Finite-time Lyapunov dimension and hidden attractor of the Rabinovich system. *Nonlinear Dyn* 2018. <https://doi.org/10.1007/s11071-018-4054-z>.
- [37] Laarabi H, Abta A, Hattaf K. Optimal Control of a delayed SIRS epidemic model with vaccination and treatment. *Acta Biotheor* 2015;63(15):87–97.
- [38] Lin Q, et al. A conceptual model for the coronavirus disease 2019 (COVID-19) outbreak in Wuhan, China with individual reaction and governmental action. *Int. J. Inf. Dis.* 2020;93:211–16.
- [39] Mahdy AMS, Sweilam NH, Higazy M. Approximate solutions for solving nonlinear fractional order smoking model. *Alexandria Engineering Journal* 2020;59(2):739–52.
- [40] Nababan S. A filippov-type lemma for functions involving delays and its application to time-delayed optimal control problems. *optim. Theory appl* 1979;27:357–76.
- [41] Sene Ndolane. SIR epidemic model with Mittag-Leffler fractional derivative. *Chaos, Solitons and Fractals* 2020;137:109833. 2020 <https://doi.org/10.1016/j.chaos.2020.109833>.
- [42] Sene Ndolane. Second-grade fluid model with Caputo-Liouville generalized fractional derivative. *Chaos, Solitons and Fractals* 2020;133:109631. 2020 <https://doi.org/10.1016/j.chaos.2020.109631>.
- [43] Sene Ndolane. Fractional diffusion equation with new fractional operator. *Alexandria Eng.J.* 2020. <https://doi.org/10.1016/j.aej.2020.03.027>.
- [44] Sweilam NH, Al-Mekhlafi SM. Optimal control for a nonlinear Mathematical model of tumor under immune suppression a numerical approach. *Optimal Control Applications and Methods* 2018;39:1581–96.
- [45] Sweilam NH, Al-Mekhlafi SM, Baleanu D. Optimal control for a fractional tuberculosis infection model including the impact of diabetes and resistant strains. *J Adv Res* 2019;17:125–37.
- [46] Sweilam NH, Saad OM, Mohamed DG. Fractional optimal control in transmission dynamics of West Nile model with state and control time delay a numerical approach. *Advances in Difference Equations* 2019;210:1–25.
- [47] Sweilam NH, Saad OM, Mohamed DG. Numerical treatments of the transmission dynamics of West Nile virus and its optimal control. *Electonic journal of Mathematical Analysis and Applications* 2019;7(2):9–38.
- [48] Ogren P, Martin CF. Vaccination strategies for epidemics in highly mobile populations. *Appl. Math. Comput.* 2002;127:261–76.
- [49] Podlubny I. Fractional differential equations. London: Academic Press; 1999.
- [50] Ruan S, Xiao D, Beier JC. On the delayed ross-macdonald model for malaria transmission. *Bull. Math. Biol.* 2008;70:1007–25.
- [51] Silva CJ, Torres DF. Optimal Control strategies for tuberculosis treatment: a case study in angola. *Numer. Algebra Control Optim.* 2012;2(3):601–17.
- [52] Velavan TP, Meyer CG. The COVID-19 epidemic. *Trop. Med. Int. Health* 2020;25:278–80.
- [53] Wang W, Khan MA. Analysis and numerical simulation of fractional model of bank data with fractal-fractional Atangana-Baleanu derivative. *J Comput Appl Math* 2019;2019:1–23.
- [54] WHO. Coronavirus disease 2019 (COVID-19). Situation Report 126 WHO; 2020.
- [55] Wolf A, Swift JB, Swinney HL, Vastano JA. Determining lyapunov exponents from a time series. *Physica D: Nonlinear Phenomena* 1985;16(3):285–317.
- [56] Wu J, et al. Estimating clinical severity of COVID-19 from the transmission dynamics in Wuhan, China. *Nat. Med.* 2020;26:506–10.
- [57] Wu Z, McGoogan JM. Characteristics of and important lessons from the coronavirus disease 2019 (COVID-19) outbreak in China: summary of a report of 72,314 cases from the Chinese center for disease control and prevention. *JAMA* 2020;323:1239–42.
- [58] Zaman G, Kang YH, Jung JH. Optimal treatment of an SIR epidemic model with time delay. *Biosystems* 2009;98(1):43–50.
- [59] Mahmoud Emad E, Higazy M, Al-Harthi Turkiah M. Signal flow graph and control of realizable autonomous nonlinear Chen model with quaternion variables. *Alexandria Engineering Journal* 2020 DOI: <https://doi.org/10.1016/j.aej.2020.02.021>.